ANALYSIS OF SECANT PILE WALL AS DEEP EXCAVATION SUPPORT SYSTEM IN SILTY SAND SOILS INCASE OF HAWASSA TOWN

A Thesis Submitted to

School of Graduate Studies of Adama Science and Technology University

In Partial Fulfillment of the Requirement for the Degree of

Master of Science in Civil Engineering

By: **HIYAW HATIYA**

Advisor: **HENOK FIKRE (Dr.ING)**

JUNE 2016

Adama, Ethiopia.

Analysis Of Secant Pile Wall As Deep Excavation Support System In Silty-Sand Soils In Case Of Hawassa Town

ADAMA SCIENCE AND TECHNOLOGY UNIVERSITY

SCHOOL OF GRADUATE STUDIES

ANALYSIS OF SECANT PILE WALL AS DEEP EXCAVATION SUPPORT SYSTEM IN SILTY- SAND SOILS INCASE OF HAWASSA TOWN

By HIYAW HATIYA

JUNE 2016

Approved by Board of Examiners

Dr.ING Henok Fikre		
Advisor	Signature	Date
Dr. Addis allem Zeleke		16 June 2016
External Examiner	Signature	Date
Dr. Argaw Asha		17 June 2016
Internal Examiner	Signature	Date
Abda Berisso		20 June 2016
Chair-man	Signature	Date
Gemechis Kebede Likasa Civil Engineering Department Head		June 20, 2016
Chairman, Dept.'s	Signature	Date
Lemma Beressa Gudeta School Of Civil Engineering & Architecture, Dean		21/06/2016
School Dean	Signature	Date
PG Studies	Signature	Date

Adama Science And Technology University June 2016 Page i

ACKNOWLEDGEMENTS

I would like to thank the almighty GOD for all the blessings I have received during my research work and the strength he gave me through my life time.

Secondly, I would like to express my sincere gratitude to my advisor Henok Fikre (Dr. ING) for his close supervision, constructive suggestions, provision of necessary information, his guidance and encouragement throughout my work.

Thirdly, I would like to use this chance to express my recognition to ADDIS GEOSYSTEMS for providing me the necessary data's. They were very cooperative whenever I need any materials.

Lastly, I would like to thank my family and my friends for their support. This would not been possible without their support and sacrifice under very difficult circumstances. In addition, I would like to thank to my colleagues who give a lot in their positive advice during this research.

TABLE OF CONTENTS

LIST OF SYMBOLS AND ABBREVIATIONS

SPT	Standard Penetration Test;
FEM	Finite Element Model;
SNNPR	Southern Nations Nationalities and Peoples' Region;
CSA	Central Statistical Agency;
CFA	Continuous Flight Auger;
ASTM	American Society for Testing Materials;
c	Cohesion;
C increment	Increment in cohesion;
D_{ex}	Excavation Depth;
E	Elastic modulus;
e_0	void ratio;
EA	Normal stiffness;
EI	Flexural rigidity;
E increment	Increment in Elastic modulus;
FE	Finite Element;
He	Final excavation depth;
HSM	Hardening soil model;
I	Moment of inertia;
Ka	coefficient of Active earth pressure;
K	Soil modulus;
K0	initial earth pressure ratio;
Lb	Bond length;
L*s*	horizontal anchor spacing;
M	wall bending moment;
MCM	Mohr Coulomb Model;
P	Load intensity;
PIZ	Primary Influence Zone;
P*v*	Pressure;
Q	Axial load in the wall;

qs	Distributed surface load;
R*d*	Design resistant force;
RL	Reduced level;
SIZ	Secondary Influence Zone;
Sr	relative wall stiffness;
t	Thickness;
TSA	Total Stress Automatic;
w	Weight;
X	Distance;
y	Wall horizontal deflection at depth z;
yref	Reference depth;
Z1	Start depth;
Z2	End depth;
ϕ	Angle of internal friction;
ɣ	Unit weight;
δhm	maximum lateral wall deflection;
δvm	maximum ground settlement;
Ψ	Dilatancy angle;
ɣbulk	Bulk unit weight;
ɣ*r*	Partial factor;
τ	Shear stress;
σ	Compressive stress;
$\Delta\sigma_h$	Increase in lateral earth pressure;
ʋ	poisons ratio; and
ɣ sat	Saturated unit weight.

LIST OF TABLES

LIST OF FIGURES

ABSTRACT

Control of soil deformation is critical for deep excavation in crowded urban areas to minimize its effect on adjacent structures. Therefore, analysis and parametric study is important for accurately represent the response of the soil to excavation and to predict the magnitude and pattern of ground movement. This thesis presents the analysis of secant pile walls as deep excavation support system in silty sand soils. The objective of this study is to investigate and realistically simulate the effect of different parameters on the prediction of ground movement by numerical analysis and to develop a method of estimating these effects quantitatively. Relevant literatures published in the past were extensively conducted in order to understand the trends and the key developments in this area. It was revealed from the literature review that the concurrent use of the observational method and the finite element method for monitoring and controlling of ground deformations around the excavation has become a norm for deep excavation projects

During analysis Parametric study was conducted for the effect of surcharge and its location on horizontal displacement, vertical deformation and bending moment of the supporting system.

From the study, analysis results and discussions are presented with details of constitutive models used during deep excavation and provide helpful first estimation of probable damage caused on adjacent structures due to excessive excavation was also presented. Lastly, Recommendations for future works are presented.

Key words: deep excavation, secant pile wall, plaxis 2D and Harding soil model

CHAPTER ONE: INTRODUCTION

1.1 Background

Current construction of high rising building and utilities infrastructure in urban environments frequently involves the construction of deep excavation due to the need of space for commercial uses, storage, parking and others. However, experiences shows that deep excavation should be designed to have high stiffness to comply with strict specifications on the limitation of ground movements induced by excavations in congested urban areas. The failure of an excavation may result in catastrophic consequences, and to avoid such failures special care must be taken.

Deep excavations for building basements require retaining systems to support the peripheral subsoil and exclude groundwater. The type of the retaining wall used influenced by the sub-structure construction method, and will vary geographically due to soil and groundwater conditions, proximity to the source of materials, and the skill of local contractors. Various types of retaining systems are categorized according to the above reasons and others. Deep excavation manual (1996) provides a comprehensive review of various types of retaining systems such as sheet walls, diaphragm walls, braced walls, contiguous pile walls, secant pile walls and others.

Secant pile walls have been widely used as primary structural elements for supporting deep excavations in urban areas due to their structural advantages and designed with respect to their lateral displacements, which can be reduced by adopting a stiffer wall, by reinforcing the anchor or strut system, or by pre-stressing these components.

Deep excavations represent a complicated soil-structure interaction problem. It is, therefore, essential to make optimum use of previous experience and case histories in similar conditions, e.g. the empirical methods proposed by Peck (1969) and Clough and O'Rourke (1990) cannot always provide reasonable prediction on the deformation pattern in current modern construction in terms of construction sequence, anchor system and development of pore water pressure. In addition, obtaining similar relationships using the empirical approach is rather difficult, since capturing the isolated effects of the various factors requires a significant number of well documented and controlled case studies. Assessing and analyzing such a large number of case studies are difficult.

Numerical modeling is an effective way to investigate the performance of deep excavations; many constitutive models have been developed to represent the soil behavior over the past decades, for example, elastic-perfectly plastic model and hyperbolic model. The selection of the most suitable constitutive model is very crucial in insuring safe and economical design. It requires a deep understanding of soil mechanics, constitutive modelling and nonlinear numerical methods, as well as familiarity with the algorithms implemented in the software to be employed for the analysis (Potts and Zdravkovic 2001).

Taking Hawassa town as a case study this thesis demonstrates an application of PLAXIS. It incorporates constitutive models, whose parameters obtained either directly or through correlation from simple tests, e.g. SPT test.

1.2 Objectives of the research

The objective of this research is to gain insight into the analysis of deep excavation taking secant pile wall as support system and determine the suitability as deep excavation support system.

The specific objective of this work includes:

- ✓ Analysis of secant pile wall as a deep excavation support system in silty sand soils.
- ✓ Provide helpful first estimate of probable damages caused on adjacent structures due to excessive excavation.

1.3 Scope and limitation of the study

The main goal of this thesis is to analyze secant pile wall as deep excavation support system including parametric study in silty sand soil in case of Hawassa town using PLAXIS 2D finite element software. Additionally to facilitate the implementation of secant pile wall in Hawassa Town. The data and parameters, which obtained from the field studies, will be evaluated in all manner of how they affect the ground deformation. Thus by using the field data and study results the probable and predictable ground deformations can be estimated. The results from this research can be used in estimating the possible damage that will be caused if support systems were not introduced. Hence, possible measures can be taken to reduce the problems arising to the new structures and existing structures during and after construction. Hawassa town is chosen due the presence of investors' and booming of complex structure in the Town.

As in most studies that attempt to correlate different engineering parameters, the size and quality of the data is the main factor that limits the applicability of the result obtained. In addition, some facts should be considered in the study.

1. A secant pile wall is required for controlling horizontal ground movements resulting from deep excavation. However, when choosing a support system for the deep excavation, it should be kept in mind that even the secant pile wall will result in some horizontal displacement of the ground. Therefore, selecting a secant pile wall alone does not eliminate all the horizontal ground movements.
2. Since PLAIXS 2D ignores the corner effects of excavation on deformation and bending moment, its effective to use PLAXIS 3D for further analysis.

1.4 Methodology

The available literature in the area of study is assessed to establish the factors that affect the analysis of a secant pile wall as deep excavation support system. Suitable finite element software is then employed to determine the different parameters that play important role in the design of secant pile walls and parametric study is then conducted to establish the significance of each parameter.

Apparent earth pressure diagrams proposed by Peck (1969) are used to calculate strut loads, and are not valid for the calculation of bending moments in the excavation support wall. The trapezoidal pressure diagram is used for anchor load determination for medium dense to very dense sands. A proper understanding of soil-structure interaction is vital to the efficient, accurate and cost effective design of excavation support systems. Hardening Soil model is used for analysis and simulation of the non-linear, time dependent and anisotropic behavior of soils provided as a special features.

1.5 Structure of the thesis

The thesis consists of five chapters. The first chapter describes the background information of deep excavations. The previous studies and recent progress in the analysis of deep excavation including the theoretical, empirical and numerical analyses discuss in the second chapter. Chapter three labels the study area and the base model parameters used for analysis purpose in the next chapter. The fourth chapter is outlines the different parameters and results of the analysis done. And chapter five summarizes the work of previous chapters and gives some general conclusions and recommendations for possible future work.

CHAPTER TWO: LITERATURE REVIEW

2.1 Introduction

A variety of excavation methods and lateral supporting systems are to be practiced based on local soil, ground water and environmental conditions, allowable construction period, money and machinery. Excavation methods include full open cut methods, braced excavation methods, anchored excavation methods, island excavation (partial excavation) methods, and top-down construction methods and zoned excavation methods. Types of deep vertical soil support systems are commonly used in metropolitan cities are Conventional retaining walls, Soldier pile with wooden lagging walls, Sheet pile walls, Diaphragm walls and Pile walls-Contiguous, Secant or Tangent. Apart from retaining walls to resist lateral earth pressure a supplementary strutting systems are also required. A strut is made of wood, reinforced concrete or steel. Based on function of a strut, it may classify as an earth berm, a horizontal strut, an anchor or as a top-down floor slab. During construction of excavation supporting system, the adjacent facilities can be damaged. Vibration due to adjacent machinery, vehicles, rail-roads, blasting and other sources require that additional bracing precautions are to be taken. This may avoided by taking some ground improvement measures such as grouting the ground between the excavation site and adjacent building.

One of the recent deep excavation support system are Secant Pile Walls and formed by constructing intersecting piles by keeping the spacing of piles less than diameter. Secant pile walls are used to build cut off walls for the control of groundwater inflow and to minimize movement in weak and wet soils. They are constructed in the form of hard/soft or hard/firm and Secant Wall Hard/hard wall. Secant Wall-hard/soft or hard/firm is similar to the contiguous bored pile wall but the gap between piles is filled with an unreinforced cement/bentonite mix for the hard/soft wall and weak concrete for the hard/firm wall. Construction is carried out by installing the primary piles (A) and then the secondary piles (B) are formed in reinforced concrete, cutting into the primary piles, diameters can range from 400mm to 1200mm. Secant Wall Hard/hard wall construction procedure is very similar to a hard/firm wall but in this case the primary piles (A) are constructed in high strength concrete and may be reinforced. The Secondary piles (B) are cut into the concrete primary piles (A) using heavy duty piling rigs fitted with specially designed cutting heads. Secant pile walls are stiffer than tangent piles walls and are more effective in keeping ground water out of the excavation.

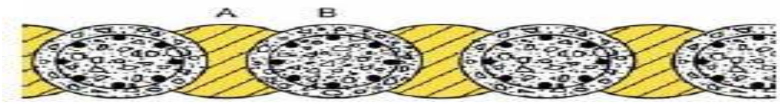

Secant Wall – hard/soft or hard/firm

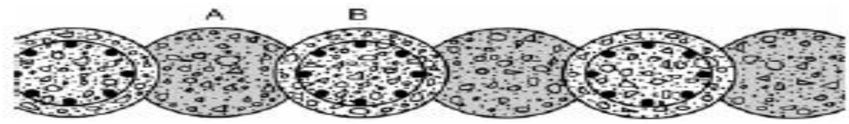

Figure 2-1: Secant pile wall scheme (venkata et al., 2011)

Secant pile walls can be constructed using several different drilling methodologies, depending on ground conditions, pile diameters, retaining heights and site access. It is important to note that for all Continuous Flight Auger (CFA) techniques computer monitoring of the pile installation process is essential for quality assurance:

- Continuous Flight Auger (CFA) piles for primary and secondary piles
- CFA piles for primary piles and rotary bored piles with thick walled segmental casings for secondary piles
- CFA piles for primary piles and cased CFA (CCFA or CSP) for secondary piles
- Rotary bored piles with standard thin walled temporary casing for primary piles and rotary bored piles with thick walled segmental casings for secondary piles

It is critical to select a suitable drilling methodology for the secondary or “male” piles to achieve sufficient interlocking between the piles. Loose joint connecting the

CFA auger sections or the drill auger to the Kelly bar could cause lack of rigidity of the drill string resulting in undrained deviations.

CFA piles require constant penetration rates to avoid uncontrolled, lateral spoil removal during the drilling process. Particularly in inner-city projects with adjacent structures and building in close proximity to the proposed secant pile wall, uncontrolled spoil excavation by the CFA auger can cause severe settlements and damages on the adjacent structures.

This chapter is classified in the following categories: approaches to design and analysis of deep excavation support system, earlier works, numerical studies of deep excavations and Field performances study of deep excavations

2.2 Approaches to design and analysis of deep excavation support system

The deep excavation is a complex subject in geotechnical engineering and has been studied using various methods, e.g. theoretical and empirical methods, laboratory tests, field measurements, and more sophisticated numerical analysis. However, all these methods have their limitations, although they have contributed in various degrees to the understanding of the performance of deep excavations. Theoretical and empirical methods provide some basic understanding of the performance of deep excavations in a different way, but they also have limitations due to their simplicity and assumptions. Some of these methods are reviewed in this section. The common approaches in analysis and design of deep excavation support systems are the Analytical model, spring model and the Finite element model

Analytical method is based on some classical theories that determine the stresses on a retaining structure for the cases of active and passive earth pressure. Design of retaining walls requires the evaluation of active earth pressure, which is largely based on the classic solutions of lateral earth pressure provided by Coulomb (1776) and Rankine (1857). Coulomb (1776) first studied the earth pressure problem using the limit equilibrium method to consider the stability of a wedge of soil between a retaining wall and the failure plane. It is well verified for the frictional soil in active state, but is not the case either for the cohesive soil or for the passive state. Rankine (1857) presented a solution for lateral earth pressures in retaining walls based on the plastic equilibrium. He assumed that there is no friction between the retaining wall and the soil, the soil is isotropic and homogenous, the friction resistance is uniform along the failure surface, and both the failure surface and the backfilled surface are planar.

Analytical method used today, but they are only applicable under certain conditions to estimate roughly the earth pressures on the wall. Moreover, they do not consider the construction process and give no indications on the wall deformations and ground movements in the more complex braced deep excavations.

Spring model is the other approach for a deep excavation analysis. This theory focuses on the bending of a beam resting on an elastic foundation and assume the force acting on the retaining structure can create soil pressure and deformation change. It is a coupled process as the excavation induces unbalanced force against retaining structure and causes change in stress state and deformations, and these changes in return affect the unbalanced force. Compared to analytical models, numerical models can simulate and solve more complex conditions, as the computer can easily take over the calculation process. One of the most widely used geo-technical software for retaining wall design in Netherlands, D-Sheet piling, is based on this beam on elastic foundation theory.

Compared to the analytical method, the spring model simulates the soil structure interaction accordingly with the deflection of the retaining structure. Therefore, it provides simulation that is more realistic. Moreover, the model is easily adopted by computer program, which makes the calculation done in a very short period. These advantages make the spring model the most popular model in the practical retaining structure design, especially when the structure is not very complex. The spring model also has its limitations. It is an analysis method based on the plane strain condition. Nevertheless, in reality, the excavation on the short side of the building pit will be affected by the corner effect, and result in smaller deformation compared to plane strain condition.

The finite element method, FEM, consists of modeling the wall and the soil as made of small elements and assigning to the elements properties, which control their behavior. Beam elements are usually chosen to represent the wall while brick elements are used for the soil. The finite element method is capable of simulating the change of soil pressure, structure deformation, and groundwater pressure. However, it is merely simulates the problem numerically. It is still down to the proper geotechnical theories applied that solve the problem. Moreover, modern commercial FE software provides rather vigorous solutions. It requires analysts' knowledge and experience to make sure the model is built up correctly and properly translated when the result presents.

As mentioned in previous sections, a major advantage of finite element method is that the model has more realistic approximation for the change of deformation of soil and structure, as well as the change of stress state accordingly. For a complete theoretical solution, the following four conditions should be satisfied: Equilibrium; Compatibility; Material constitutive behavior; Boundary conditions. The analytical model is not able to fulfill all these conditions at the same time. In addition, it does not provide information on movements or structural forces under working load conditions. Simple numerical methods, such as the beam-spring approach, can provide information on local stability and on wall movements and structural forces under working load conditions. However, they do not provide information on overall stability or on movements in the adjacent soil and the effects on adjacent structures. Full numerical analysis, for instance the FEM, can provide information on all design requirements.

2.3 Earlier Works

Chavda et al (2014) presented numerical modeling of pile wall using PLAXIS -3D in order to carry out parametric studies, effect of stage wise excavation on the ground and pile wall deformation. The length of wall is taken as 16m, diameter of pile as 750mm, Capping beam of 750 x 375 mm considering same properties of pile, height of excavation is up to 8m with stage-wise excavation of every 2m, 3D model of 30m x 3m x 20m (X, Y & Z) having pile wall at distance of 20m. In order to discard the effect of pore water pressure, modeling (Mohr-Coulomb) is done considering no water table i.e. dry soil. The stage wise excavation is done in phases to stimulate actual site condition on field. The depth of excavation in each phase is of 2m with total 4 phase, excavation depth of 8m is done. The first parametric studies carried out varying the soil friction angle, the soil friction angle used in the previous section is 30˚. Therefore, model of Φ=30˚ is used as the control model. The values of Φ used in this part are 20˚, 25˚, 30˚, 35˚ and 40˚. Second parametric study is carried out by varying the unit weight of soil. Similar to the first parametric study, PLAXIS model in pervious section with unit weight of 16KN/m^3 is used as control model. In this study, the unit weights used is 14, 15, 16, 17 and 18KN/m^3. The third parametric study is height of wall. In control model from pervious section, the height of wall used is 16m. The values of height of wall used are 14, 15, 16, 17 and 18m for parametric study. The last parametric study conducted based on diameter of pile by increasing from 750 to 1500mm.

Based on the method used and output results Chavda et al (2014) conclude the following.

- With progress in excavations, the ground deformation increases and the settlement value becomes larger and larger as the excavation deepens. According to numerical analysis, a distance range of 0 m to 10 m from the foundation excavation is the main influence area, and then away from the excavation, there is less influence on surface settlement.

- In parametric studies, when soil friction angle increases, the deformation of Pile wall decreases, this is due to the increasing internal shear strength within the soil with increasing soil friction angle. Hence, active earth pressure developed on the wall is reduced.
- When the soil unit weight increases the deformation of Pile wall increases. When soil unit weight increases, vertical stress acting on a soil mass increases, and eventually causes lateral active stress to increase.
- With increase in height of Pile wall from 14m to 17m, there is decrease in deformation of pile wall. Ata wall height of 18m there is increase in deformation of pile wall is observed, this is due to increases in slenderness ratio and it cannot take passive resistance from the bottom portion of pile wall when it rotates.
- With increase in diameter of pile reduces the deformation of pile wall. This is due to increase in structural stiffness.

Zhou (2015) discussed the use of 3D finite element method in deep excavations, especially the simulation of sequential excavation method in 3D FEM model. Spaarndammer tunnel project in Amsterdam was used as study area and the soil parameters used in the models were derived from in-situ soil investigation. Cone penetration tests and boreholes were carried out along the tunnel location. Parametric study has been done in order to investigate how the domain and mesh set-up influence the results in 3D FEM model. Comparisons were done between 2D and 3D FEM by taking certain geometry of excavation section. Also after comparison, the sequential excavation method was implemented into 3D FEM model. Different excavation rates, excavation directions and lateral support design were tested in order to optimize the sequential excavation model. The response of sheet pile walls as well as surrounding soil were recorded and compared with the results from normal 3D excavation model.

Based on the parametric studies results he concluded the following

- When the excavation section is longer than 50m, the whole domain can be considered as plain strain, so that the results in 2D and 3D FEM models were almost the same.
- When the section lowered from 50m to 30m the bending of sheet pile wall reduced by 20% due to the corner effect in 3D scenario. The settlement and the heave at the bottom of excavation pit were also reduced significantly.
- On the other hand, the deflection of sheet pile wall and settlement from the normal staged excavation models were well within the range of acceptance, but the improvement was not as striking as expected. The excavation is almost 10 meter on one side, but the difference of deflection results is only 1.5 cm. The difference is almost negligible in practice.

Peck (1969) considered deep excavations to be excavated with vertical sides that require lateral support. Lateral movements, ground settlements next to excavations, base failure by heave, methods for reducing ground settlement next to excavations, and earth pressure diagrams for deep excavation design were the main topics discussed by peck. There were three major themes in peck's discussion of deep excavations the importance of soil type and the properties on the performance of deep excavations, the importance of the deep excavation and the importance of what peck called "workmanship" in controlling movements. Workmanship includes factors such as prompt installation of supports.

He developed the first empirical method to predict the wall movement based on actual ground deformation data collected from temporary braced sheet pile and soldier pile walls with tie back support as shown in Figure 2.3.1.

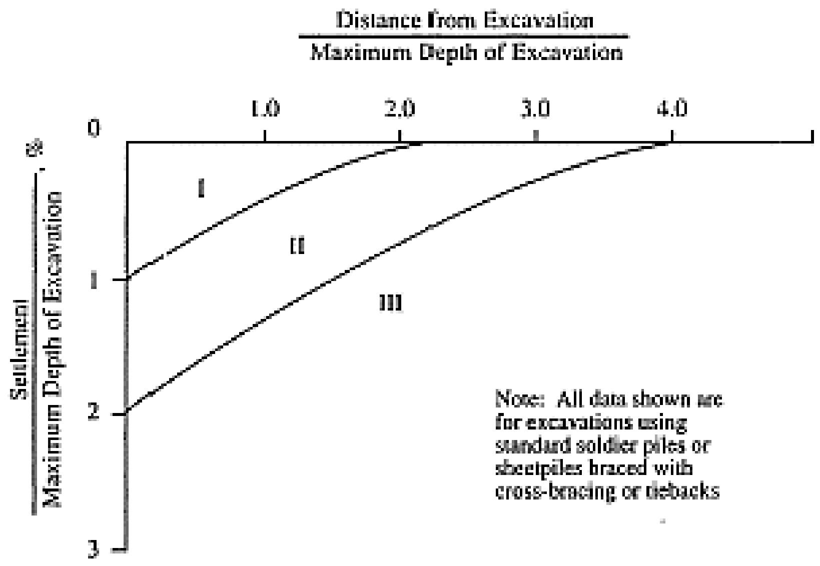

Figure 2-2: Summary of Settlements adjacent to open cuts in various soils as a function of distance from edge of excavation [Peck, 1969]

Zone I Sand and Soft to Hard Clay average workmanship

Zone II a) Very Soft to Soft Clay

(1) Limited depth of clay below bottom of excavation

(2) Significant depth of clay below bottom of excavation but Nb < Ncb

b) Settlements affected by construction difficulties

Zone III Very soft to soft clay to a significant depth below bottom of excavation and with $N_b > N_{cb}$

The stability number N_b is defined as $\gamma H / S_{ub}$, where γ is the unit weight of the soil above the base of excavation, S_{ub} is the undrained shear strength below the base of excavation, and N_{cb} is the critical stability number for basal heave. Terzaghi (1943) as follows in Figure 2.3.2 defined the factor of safety against basal heave.

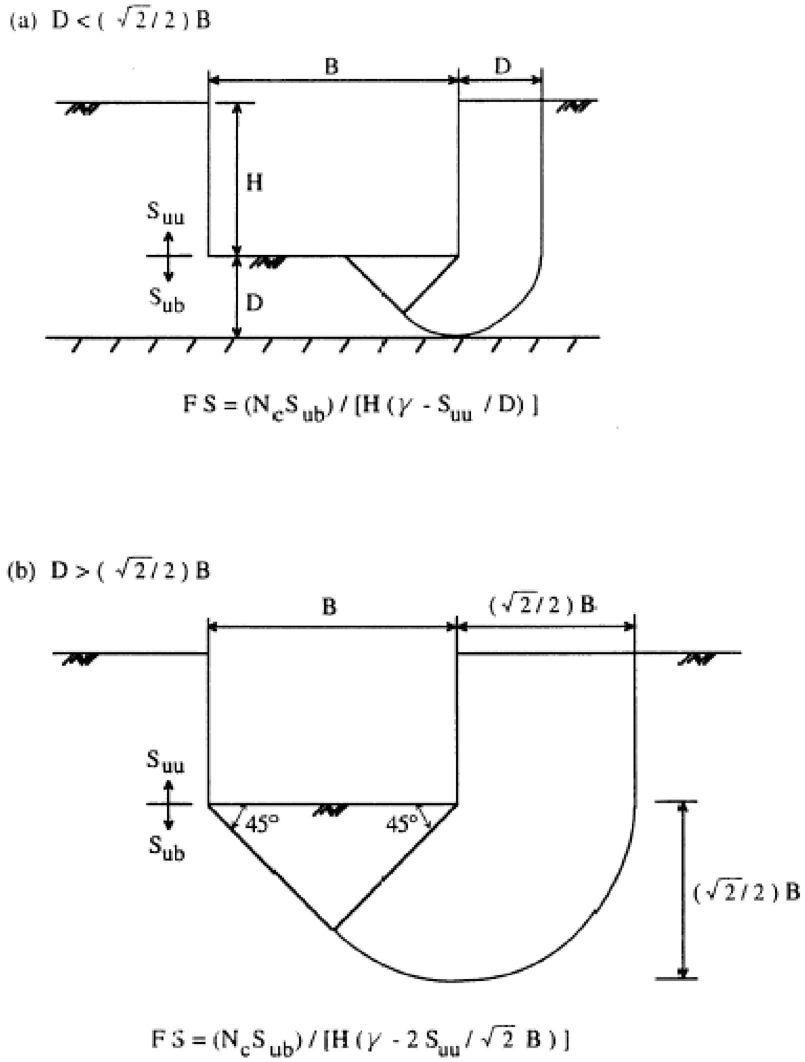

Where:

D = distance between the base of excavation and hard stratum

B = width of excavation

N_c = bearing capacity coeffiecient

S_{ub} = undrained shear strength below the base of excavation

S_{uu}= undrained shear strength above the base of excavation

γ = unit weight of soil

Figure 2-3: Excavation geometry and soil strength parameters for factor safety against basal heave (Terzaghi, 1943)

The chart, Figure 2.3.2, can be used to predict the ground deformation which can extend up to four times the excavated depth from the wall. However, since it was based on data collected from excavations less than about 15 meters depth with relatively flexible retaining walls, there would be uncertainties in extrapolating these observations to much deeper excavations supported by diaphragm walls.

Clough and O'Rourke (1981) studied the movements due to deep excavations by examining information from case histories and previous studies. They presented the current state of the art of empirical observations for estimating the lateral wall deflections and surface settlements in excavations. They divided movements into two types. One was movement due to the excavation and support process, and the other was movement caused by auxiliary construction activities. They summarized movement information from case histories to aid in estimating maximum wall movements and settlement profiles of the ground next to excavations. They concluded from their study that movements due to deep excavations could be predicted within the reasonable bounds if the significant sources of movement were considered. Based on the result the following conclusions were made.

- The maximum lateral wall deflections and maximum surface settlements were usually less than 0.5%H.
- The maximum lateral wall deflections tended to average about 0.2%H.
- The maximum surface settlements tended to average about 0.15%H.

Hsieh and Ou (1998) suggested that there were two types of settlement profiles caused by excavations: (i) spandrel type, in which maximum settlement occurs very close to the wall; and (ii) concave type, in which maximum settlement occurs at a distance away from the support wall. The spandrel type of settlement profile occurs if a large amount of wall deflection occurs at the first stage of excavation when cantilever conditions exist and the wall deflection was relatively small due to subsequent excavation. After the initial stages of excavation, additional cantilever wall deflection was restrained by installation of support as the excavation proceeds to deeper elevations. The concave settlement profile reflected the ground settlement profile that developed when the movements were more deep-seated.

They presented the relationship shown in Figure 2.3.3 for a spandrel-type condition. The data were presented as normalized settlement, $\delta v/ \delta vm$, where δ_{vm} maximum ground surface settlement, versus the square root of the distance-from-the-edge-of-the-excavation divided by the-excavation-depth (d/He). This relationship was based on 10 case histories from Taipei, Taiwan. The "mean" estimate curve shown in the figure was derived based on the results of regression analysis.

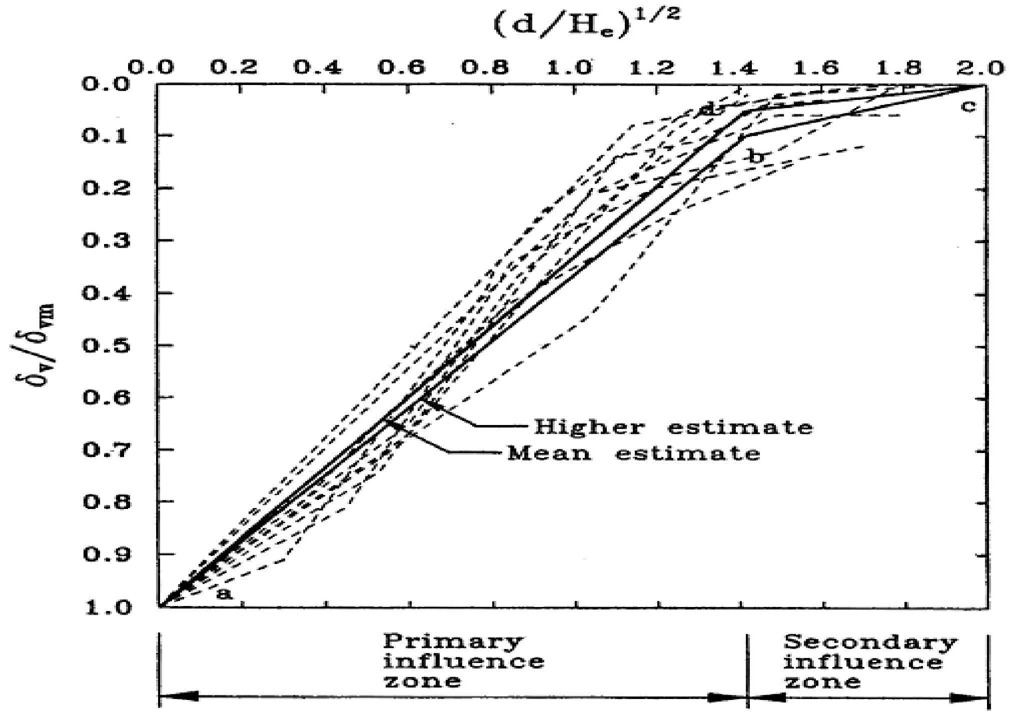

Figure 2-4: Shape of “Spandrel” Settlement Profile (After Ou et al., 1993).

Balasubramaniam et al (1994) analyzed the performance of six deep excavations with different support systems and construction methods in Bangkok sub-soils. Parametric finite element studies of the effects of pre-loading, barrette pile and foundation pile and foundation pile installation, embedment depth, and surcharge are also presented. Analytical results agreed in general with the observed behavior and they concluded that the stiffness of the retaining wall and bracing element control deformations. They also found that diaphragm walls performed better (smaller movements) than sheet pile walls and wall embedment depth was a more significant performance factor with sheet pile walls than diaphragm walls.

2.4 Numerical studies of deep excavations

Hoe N. H. (2007) carried out a parametric study using finite element method to investigate the effects of soil stiffness, the initial coefficient of lateral earth pressure and rock socket length. They also investigated the suitability of constitutive models (Hardening Soil model and Mohr-Coulomb model) by comparison with field monitored measured data. They used PLAXIS V-8 employing plain strain assumption and wished-in-place diaphragm wall. From the study, they concluded that wall deflection was very sensitive to change in soil stiffness and coefficient of lateral earth pressure. Through comparison with measured field monitored data, it was observed that Hardening Soil model can predict ground deformation more precisely than Mohr-Coulomb model.

Whittle et al. (1993) described the application of a finite element analysis for modeling the top down construction of a seven-story, underground parking garage at post office square in Boston. The analysis incorporated coupled flow and deformation within real time simulation of construction activities. Predictions were evaluated through comparison with extensive field data, including settlement, wall deflection, and piezometric elevations. Good agreement was obtained but it was emphasized that adequate characterization of engineering properties for the entire soil profile was important.

Jen (1998) carried out extensive parametric studies to investigate how predictions of excavation-induced ground movements were related to key parameters such as excavation geometry, support system and soil mass stress history profile. Depth of bedrock was found to be the key parameter affecting the distribution of ground movements, excavation width, excavation depth and uncertainties in the stress history profile and support stiffness were major factors contributing to the magnitude of the displacements. The computed settlement troughs in the retained soil were described as dimensional functions of excavation depth wall length, bedrock depth and soil profile. These equations offer a new approach for geotechnical engineers to preliminary design calculations of ground movement. The hypothetical simulation results were used in later chapters of this dissertation for calibration of the mobilizable strength design method.

Powrie and Li (1991) have carried out a series of numerical analyses on excavations singly propped at the crest of the retaining wall. The effect of soil, wall and prop stiffness and pre-excavation pressure coefficient were investigated. As the structure investigated was very stiff, so the magnitude of soil and wall movements was governed by the stiffness of the soil rather than that of the wall. A reduction in soil stiffness by a factor of two resulted in an increase in wall deformation almost by the same order of magnitude. On the other hand, wall movement was little affected by a 40% reduction in bending stiffness when the thickness of the wall was reduced from 1.5m to 1.25m. The assumed pre-excavation lateral earth pressure significantly affected the prop loads and bending moment though the deformation would not increase much due to the accompanying increase in soil stiffness. The connection of the base slab to the retaining wall had an important influence on the bending moment profile of the slab. The provision of a quasi-rigid construction joint reduced the bending moment in the wall and the hogging moment at the center of the prop slab, but introduced a sagging moment in the slab at the connection to the wall.

Ramadan et al (2013) presented "analysis of piles supporting excavation adjacent buildings" in order to reduce the surrounding soil movement due to deep excavation, a 3D FEM study was carried out considering the soil-structure interaction. A piled supporting system was selected because it was common and relatively economical to use in cohesive soils in Egypt. In addition, a parametric study was performed to study the effect of the stiffness of the supporting system on minimizing the ground deformation. The soils were assumed to be deposited of clay and Mohr-Coulomb model was used for analysis. Based on the output they concluded pile wall embedded depth had no obvious effect on the stability of the supporting system for N_c value up to 4. The effect can be seen for $N_c>4$ up to H/D =1.

Surarak et al (2012) presented "stiffness and strength parameters for Harding soil model of soft and stiff Bankok clays" to determine the stiffness and strength parameters for Hardening Soil Model. In analysis, the material type of soil clusters was set to undrained that allow a full development of excess pore water pressure and a flow of pore water to be neglected. Thus, the coefficient of permeability was not required in the undrained analysis. In addition, Oedometer data were obtained from three different Bangkok soil layers. Based on the result they concluded For Soft Bangkok Clay; the angle of internal friction at the depths of 2.5–4 m can be assumed to be 26˚; this value can be reduced to 24˚ at depths of 5.5–6 m.

Usmani et al (2010) presented on Analysis of Braced Excavation Using Hardening Soil model and carried out a soil structure interaction study of a braced excavation to assess ground movements, displacements, earth pressure and bending moment distribution along the height of wall. The soils considered in the analysis were sandy silt and silty sand representing Delhi Silt with negligible plasticity. Hardening Soil (HS) model used to study the soil-structure response under the above soil types and captured the behavior of braced excavation. Usmani et al concluded the maximum positive moment was developed near the mid height of the wall and negative moments towards the lower part of the wall in both the soils considered. The bending moment at the toe level was found to be almost zero, signifying the fact that fixity did not develop there, as the penetration of the wall in the stiffer stratum is small.

Garvin, R. and Boward, J. (1992) discussed the cut-and-cover construction of a five level underground parking structure in Pittsburgh. The support selected in this case was a diaphragm wall with tiebacks for 7m to 8m excavation. Slurry wall system performed well and permitted dewatering within the excavation within a minimum influence on groundwater levels outside excavation. Maximum lateral movements for the excavation were between 10 and 20 mm. An adjacent 80-year-old sandstone structure experienced no distress. Also during construction, monitoring instruments were used for deformation and ground water levels assessment.

Raithel et al (2005) have given design and numerical investigations of a deep excavation for a tunnel entrance pit in Germany. This new shield tunnel was constructed to replace the existing bridge for the crossing of the trave river in Lübeck, Germany. The paper studied the construction and design of the retaining structures together with the 12.5 m high cofferdam using FE-program PLAXIS 8.2.

Table 2-1: Soil parameters at the excavation pit [Raithel et al, 2005]

Soil layer	Unit weight/γ′ KN/m³	Angle of internal Friction Φ′ [°]	Cohesion c′ [KN/m²]	Elastic modulus Es [MN/m²]
Sand fill	19/11	37.5˚	0	50
Upper sand	19/11	37.5˚	0	50
Basin silt	19/20	25.0˚	20	20-25
Boulder clay	22/22	30.0˚	20	30
Lower sand	19/21	37.5˚	0	50

The numerical analysis of the excavation was performed with the FE-program "PLAXIS" and a 15 node triangular element was used to generate the model mesh. An advanced constitutive soil model known as the hardening soil model (HSM) was used to simulate the soil behavior under excavation. The FE-computations were carried out for the different construction stages. The groundwater table in the upper aquifer is taken to be at a depth of 3.5 m below the surface and the lower confined aquifer at 4.5 m below the surface.

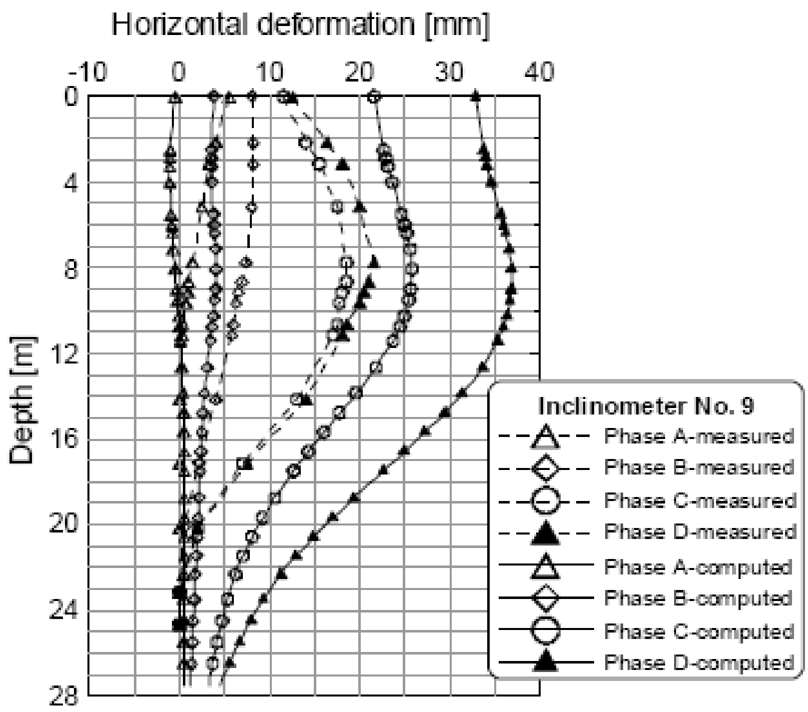

Figure 2-5: Comparison of the measured and computed deformations [Raithel et al, 2005]

Generally, the numerical results show a good agreement with the measured values, especially when the additional in-situ wall toe displacement is taken into consideration in the analysis of the inclinometer measurements. The reason for the relatively small measured deformation in comparison to the computed values may lie on the favorable geometrical in-situ situation, the possibility of an uncompleted consolidation process (excess pore pressure might still exist in some layers at the end of the excavation) and the necessary approximation of some input parameters.

Konstantakos et al (2004) conducted back analyses on an excavation up to 23m deep for the Dana Farber research tower in the Longwood medical area of Boston, which was supported by a permanent perimeter diaphragm wall using finite element software, PLAXIS 8.2. This paper summarizes the performance of the lateral earth support system based on field monitoring data measured during excavation of the basement and details of back analyses used to evaluate and interpret the wall and ground movements.

A series of finite element simulations had been carried out to obtain better insight into the performance of the excavation support system for the Dana Farber research tower. The calculations had been carried out using the PLAXIS finite element code (2002), plane strain models. Each of the soil layers had been simulated using the Hardening Soil (HS) model as it enables a realistic description of the stiffness of the retained soil relative to the excavated material with minimal additional parameters. The perimeter slurry wall was modeled using elastic beam elements (with axial and bending stiffness's; EA = 2.52x107kN/m and EI = 1.7x106kNm2/m, respectively), while elastic properties and pre-stressed loads for the rock anchors are EA = 1.0x10 kN/m.

Back-analyses of the excavation performance using PLAXIS 2-D finite element analyses were able to give consistent estimates of the measured wall deflections on each sides of the excavation.

CHAPTER THREE: STUDY AREA DESCRIPTION AND BASE MODEL PARAMETERS

3.1 Description of study area

Hawassa is a city in South Ethiopia on the shores of Lake Awassa in the Great Rift Valley. It is located 270Km south of Addis Ababa via Debr Zeit, 130Km East of Sodo, and 75Km North of Dilla. The town serves as the capital of SNNPR and is a special zone of region. Based on the 2007 census conducted by the CSA of Ethiopia, this zone has a total population of 258,808 of whom 133,123 are men and 125,685 are women.

Figure 3-1: Hawassa town Map

3.2 Parameter Identification for Base Model

One of the key elements for the analysis of deep excavation support system is identifying parameters for base model, using in-situ test or correlations of parameters. On the basis of ADDIS GEOSYSTEMS P.L.C., investigations made near Hawassa main campus and agriculture campus, from ten SPT test data a representative value of SPT test data are chosen and required soil parameter correlations are used and selected based on data quality and availability, soil profile, and consistency. In addition, some relevant parameters for the soil has taken from literatures (Teferi 2011). DIN (German standard) is used to determine the strength parameters of the soil. The soil types considered for this study are silty-sand soils from Hawassa town. Ground water level was considered in analysis and must consider during excavation and construction.

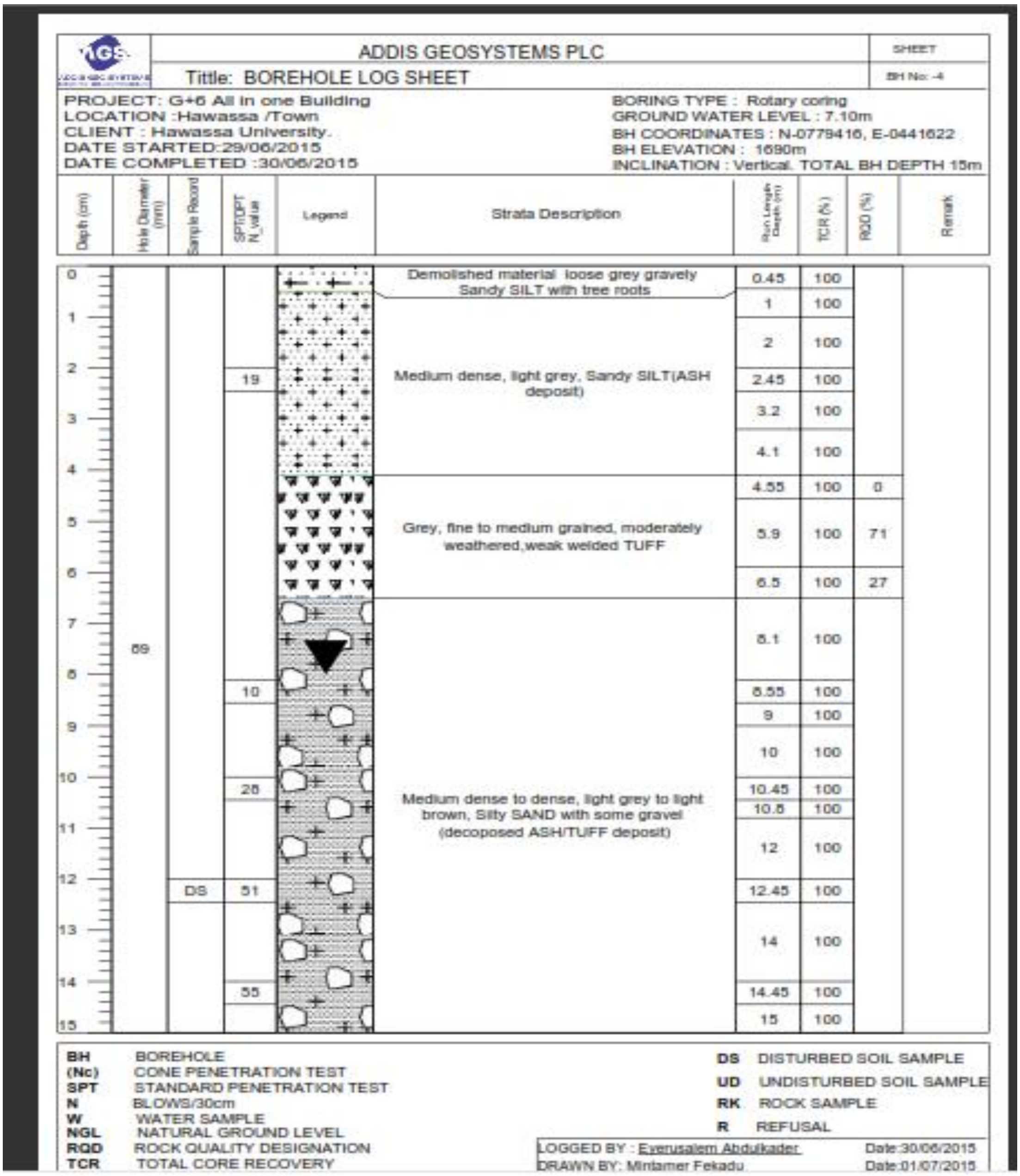

Figure 3-2: Sample borehole of Hawassa town (ADDIS GEOSYSTEM PLC)

Using DIN4094-1:4094-2 the following engineering design parameters are extracted from SPT N values and considered to represent the soil in Hawassa town.

Table 3-1: Soil Parameters of Hawassa Town

Depth (m)	SPT N_{30} (uncorrected)	Consistency	Dr	γ_{bulk} (KN/m^3)	N_{30} (corrected)	Φ (deg)
1 2	19	m. dense	0.485	18.35	24.49150813	32.25
2 4	10	m. dense	0.35	17	9.287209729	30
4 6	10	m. dense	0.35	17	8.649266556	30
6 8	10	m. dense	0.35	17	8.679629948	30
8 9	28	m. dense	0.62	19.2	23.46932389	34.5
9 11	51	v. dense	>0.85	22	41.51048526	>40
11 13	55	v. dense	>0.85	22	41.76314606	>40
13 14	55	v. dense	>0.85	22	40.47179054	>40

3.3 Lateral Earth Pressure

Peck (1943) and later Terzaghi and Peck (1969) proposed empirical pressure diagrams for wall and strut design using measured soil pressure envelopes, and can be rectangular or trapezoidal in shape. The maximum ordinate of the apparent earth pressure diagrams is denoted by p. Incorrect implementation of design earth pressure may lead to uneconomical or even unsafe designs. Traditionally, apparent earth pressure diagrams are used for designing excavation support systems. These diagrams are semi-empirical approaches back-calculated from field measurements of strut loads which do not represent the actual earth pressure or its distribution with depth. Therefore, apparent earth pressure diagrams are only appropriate for sizing the struts. As previously mentioned, the use of these diagrams yield support systems that are adequate with regards to preventing structural failure, but may result in excessive wall deformations and ground.

The trapezoidal diagram is more appropriate than the rectangular diagram for the following reasons;

- Earth pressures are concentrated at the anchor locations resulting from arching;
- Earth pressure of zero at the ground surface is appropriate for sands (provided no surcharge loading is present);
- Earth pressures increase from the ground surface to the upper ground anchor location; and
- Medium dense to very dense sands, earth pressures reduce below the location of the lowest anchor owing to the passive resistance that is developed below the base of the excavation (Aiza Malik 2015)

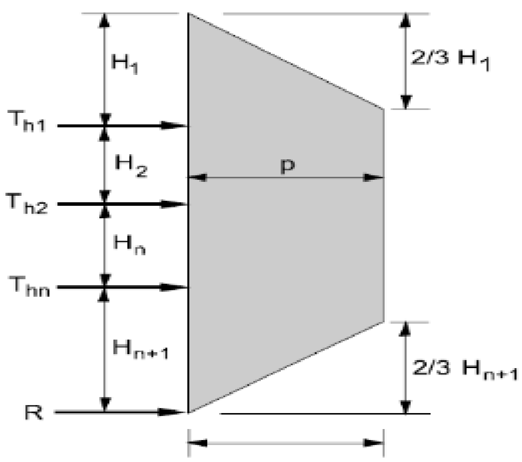

Figure 3-3: Anchor Loads for Multi - Level anchored Wall (Aiza Malik 2015)

This diagram is appropriate for both short-term (temporary) and long-term (permanent) loadings in silty-sands. Water pressures and surcharge pressures should be added explicitly to the diagram to evaluate the total lateral load acting on the wall. In this study Coulomb's Earth Pressure theory is assumed with $\delta=2\phi/3$, where δ is wall friction and ϕ is soil friction angle.

$$Pe=\frac{0.65\, tan\,^2\left(45-\frac{\phi}{2}\right)\gamma H^2}{H-\frac{H1}{3}-\frac{Hn+1}{3}} \quad \text{.........................Equation 1}$$

Where: H_{n+1}=Distance from base of excavation to lowermost ground anchor.

Thi=Horizontal load in ground anchor i.

R=Reaction force to be resisted by subgrade (i.e., below base of excavation).

P=Maximum ordinate of diagram.

γ= unit weight of soil

H= depth of excavation

H_1= Distance from ground surface to upper most ground anchor.

3.4 Water Pressures

In this paper the water table exist at 7.1m below the ground surface and it is used for in the analysis of embedment depth and for the model selected. The pore water pressure that is generated calculated.

$$p_w=\Upsilon_w*H_w \quad \text{..Equation 2}$$

Where:

p_w= pore water pressure

Υ_w=unit weight of water

H_w= depth of water

3.5 Earth Pressures due to Surface Load

With specific distance from excavation a uniform surcharge load are assumed that result in uniform increase in lateral stress over the entire height of the wall. The increase in lateral stress for uniform surcharge loading can be written as;

$$\Delta\sigma h = K^*qs \quad \text{……………………………………………Equation 3}$$

Where:

$\Delta\sigma_h$ = the increase in lateral earth pressure due to the vertical surcharge load (kPa)

q_s =the vertical surcharge stress applied at the ground surface (kPa)

K =an appropriate earth pressure coefficient.

3.6 Calculation of Ground Anchor Loads

The calculations for ground anchor loads estimated from apparent earth pressure envelopes. Methods commonly used include the tributary area method and the hinge method. Both methods, when used with appropriate apparent earth pressure diagrams, provide reasonable estimates of ground anchor loads and wall bending moments for anchored systems constructed in competent soils. In this paper, tributary area method is used for anchor load calculation.

Tributary Area Method

T1 = Load over length H1+ H2/2

T2 = Load over length H2/2 + Hn/2

Tn= Load over length Hn /2 + Hn+1/2

R = Load over length Hn+1/2

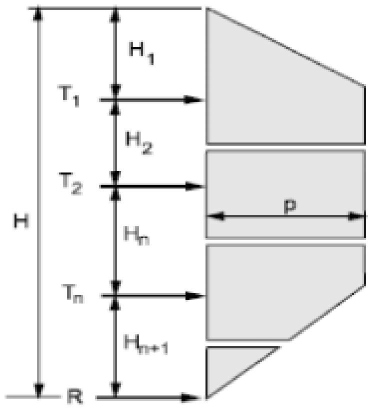

Figure 3-4: Calculation of Anchor Loads for Multi - Level anchored Wall (Aiza Malik 2015)

3.7 Soil, Pile, Diaphragm Wall and Anchor Parameters for base model

The following soil parameters are used as input for base model generation during analysis of 9, 11, and 13m excavation depth.

Table 3-2: Soil parameters for base model

depth(m	SPT N30 (uncorrected)	consistency	ɣ bulk (KN/m3)	N30 (corrected)	ϕ'(deg)	σ1'(Kpa)	c(Kpa)	Es(Mpa)
1 2	19	m. dense	18.35	24.49	32.2	36.7	2.24	70.61
2 4	10	m. dense	17	9.28	30	70.7	5.77	48.34
4 6	10	m. dense	17	8.65	30	104.7	8.54	48.62
6 8	10	m. dense	17	8.68	30	129.8	10.59	50.27
8 9	28	m. dense	19.2	23.47	34.5	139.2	5.69	79.91
9 11	51	v. dense	22	41.51	40	163.6	3.05	99.32
11 13	55	v. dense	22	41.76	40	188	3.51	102.2
13 14	55	v. dense	22	40.47	40	200.2	3.74	102.51

The selected pile diameter for base model is changed to equivalent wall thickness.

Table 3-3: Wall parameters for base model

Wall parameters	9m	11m	13m
Wall type	SPW	SPW	SPW
Adopted pile diameter	0.6m	0.6m	0.6m
Equivalent wall thickness, d	0.2826m	0.2826m	0.2826m
Normal stiffness, EA, KN/m	8.48*10^6	8.48*10^6	8.48*10^6
Flexural Rigidity, EI, KNm	5.66*10^4	5.66*10^4	5.66*10^4
Weight, w	6.78	6.78	6.78
Poisson's ratio	0.15	0.15	0.15
Pile spacing	100mm	100mm	100mm

Notes: SPW – Secant Pile Wall

EA and EI are per unit length of the wall

EA = Et, t = equivalent thickness of the pile or wall

EI = Et3/12

Anchor load calculation (sample calculation for H=9m)

The tributary area method is used to calculate the horizontal anchor loads, T1 andT2 and the reaction force to be resisted by the sub grade, Rc.

T_1=(2H1/3+H2/2)Pe+(H1+H/2)Ps = 212.56kN---------------------------- Equation 4

T_2=(H2/2+23H3/48)Pe+(H2/2+H3/2)Ps+pw1 = 159.2kN---------------- Equation 5

R_c= (3H3/16)Pe+(H3/2)Ps+pw2 = 69.78kN---------------------------------- Equation 6

Anchor design load

The inclination of all anchors is assumed to be 20^o and center-to-center spacing is taken as 2.5 m.

1. Upper anchor: The anchor design load (DL) was calculated as follows:

DL1=T1*Lc/cosΘ = 565.32kN

2. Lower anchor: The anchor design load (DL) was calculated as follows

$$DL1=T2*Lc/\cos\Theta = 423.4kN$$

The maximum calculated anchor design load is 565.32kN

Anchor capacity

The load transfer rate taken as 130KN/m, since the anchor bond zones will be formed in the dense silty sand layer. The design load with a factor of safety of 2.0 should be able to be achieved with a typical anchor bond length of 12 m, assuming a small diameter low pressure grouted anchor.

Table 3-4: Presumptive ultimate values of load transfer for preliminary design of small diameter Straight shaft gravity-grouted ground anchors in soil (Aiza Malik 2015)

Soil type	Relative density(SPT range)	Estimated ultimate transfer load
Sand and Gravel	Loose (4-10)	15
	medium dense (11-30)	220
	Dense (31-50)	290
Sand	Loose (4-10)	100
	medium dense (11-30)	145
	Dense (31-50)	190
Sand and Silt	Loose (4-10)	70
	medium dense (11-30)	100
	Dense (31-50)	130
Silt-clay mixture with low plasticity or fine micaceous sand or silt mixtures	Stiff (10-20)	30
	Hard (21-40)	60

Note: SPT values are corrected for overburden.

For a length of 12m the bond strength is

=130KN/m*12m/2 = 780kN

The allowable anchor capacity of 780 kN is larger than the maximum design load of 565.32kN. This implies that the design load can be attained at this site for the assumed anchor spacing and inclination. Right of way estimates can be made based on the bond length required for mobilization of the design load, as follows:

Maximum bond length = 565.32*2/130 = 9.55m

Tendon selection

36-mm diameters with Grade 150 pre-stressing bar have been selected based on an allowable tensile Capacity of 60 percent of the specified minimum tensile strength (SMTS). The allowable tensile capacity is 633 kN which exceeds the calculated maximum design load of 565.32 kN.

Table 3-5: Properties of pre-stressing steel bars (ASTM A722).

Steel grade	Nominal diameter	Ultimate stress f_{pu}	Nominal cross section area A_{ps}	Ultimate strength f_{pu} A_{ps}	Prestressing force		
					0.8 f_{pu} A_{ps}	0.7 f_{pu} A_{ps}	0.6 f_{pu} A_{ps}
(ksi)	(in.)	(ksi)	(in.^{2})	(kips)	(kips)	(kips)	(kips)
150	1	150	0.85	127.5	102.0	89.3	76.5
	1-1/4	150	1.25	187.5	150.0	131.3	112.5
	1-3/8	150	1.58	237.0	189.6	165.9	142.2
	1-3/4	150	2.66	400.0	320.0	280.0	240.0
	2-1/2	150	5.19	778.0	622.4	435.7	466.8
160	1	160	0.85	136.0	108.8	95.2	81.6
	1-1/4	160	1.25	200.0	160.0	140.0	120.0
	1-3/8	160	1.58	252.8	202.3	177.0	151.7
(ksi)	(mm)	(N/mm^2)	(mm^2)	(kN)	(kN)	(kN)	(kN)
150	26	1035	548	568	454	398	341
	32	1035	806	835	668	585	501
	36	1035	1019	1055	844	739	633
	45	1035	1716	1779	1423	1246	1068
	64	1035	3348	3461	2769	2423	2077
160	26	1104	548	605	484	424	363
	32	1104	806	890	712	623	534
	36	1104	1019	1125	900	788	675

Anchor base model

Table 3-6: Anchor parameters for the base model

Depth of excavation			
	9m	11m	13m
Type	Elastic	Elastic	Elastic
EA	1*10^5 KN/m	1*10^5 KN/m	1*10^5KNm
Pre-stressed load	150 KN	150 KN	150 KN
No of Anchors	2	3	4
Anchor spacing	Anchor1=3m Anchor2=3m	Anchor1=3m Anchor2=3m Anchor3=3m	Anchor1=3m Anchor2=3m Anchor3=3m Anchor4=3m

Table 3-7: Excavation and embedment depth parameters for the base model

Parameters	Unit	D_{ex1}	D_{ex2}	D_{ex3}
Depth of excavation	m	9	11	13
Depth of embedment	m	4m	3m	3m

CHAPTER FOUR: ANALYSIS AND PARAMETRIC STUDY

4.1 Introduction

There are a number of parameters to be considered if one is interested in conducting analysis and parametric study. However, as reported by earlier investigators (e.g. Chavda Jitesh, 2014), some of the variables have little or no effect in the performance of deep excavation supported by pile wall. In this paper, variables that have practical importance and reported to have significant influence in the performance of deep excavations are considered. The analysis in this paper is modeled with a geometry model of 20m width and 14 m depth and parametric study is conducted for excavation depth of 9, 11, and 13m. A combination of node-to-node anchor and Geotextiles are used in this study for the ground anchor modeling. The geotextile simulates the grout body whereas the node-to-node anchor simulates the anchor rod. In reality there is a complex three-dimensional state of stress around the grout body that can be seen in 3D PLAXIS. Although the precise stress state and interaction with the soil cannot be modeled with this 2D model, it is possible in this way to estimate the stress distribution, the deformations and the stability of the structure on a global level, assuming that the grout body does not slip relative to the soil. With this model, it is certainly not possible to evaluate the pullout force of the ground anchor. The pile wall is modeled as a beam. The interfaces around the beam are used to model soil-structure interaction effects. Interfaces should not be used around the geotextiles that represent the grout body. The excavation is constructed in several excavation stages. Geometry lines are used to model the separation between the stages.

In this paper Hardening Soil model is used and it gives precise prediction of ground deformation for deep excavations. This model is an updated version of the well-known Duncan-Chang model (Duncan et al., 1980), formulated using elasto-plasticity in which the non-linear shear-stress behavior in loading is represented by a hyperbolic function. The details of the model are presented in Appendix 1. In this paper, each of the soil types is simulated using the Hardening Soil (HS) model. Since the performance of deep excavation support system and lateral wall movements are influenced by several factors including wall installation, soil conditions, support system stiffness, ground water conditions and methods of support system installation and interaction between the soil and the support, parameters have to be identified accordingly. Finite element software PLAXIS V8.2 2D is used for analysis.

4.2 Base model generation

Representative base model and general dimensions for the study is shown in Figure 4.1. The model is simulated as a symmetrical plain strain finite element employing 15-noded triangular elements and half of the geometry with a width of 75 meters and depth of 30 meters. Surface load of 100KN/m², 120KN/m² and 140KN/m² are used during analysis. For this purpose, modeling of wall and pile, building and the soil is made using very fine mesh size. Horizontal displacement is computed at the most vulnerable location.

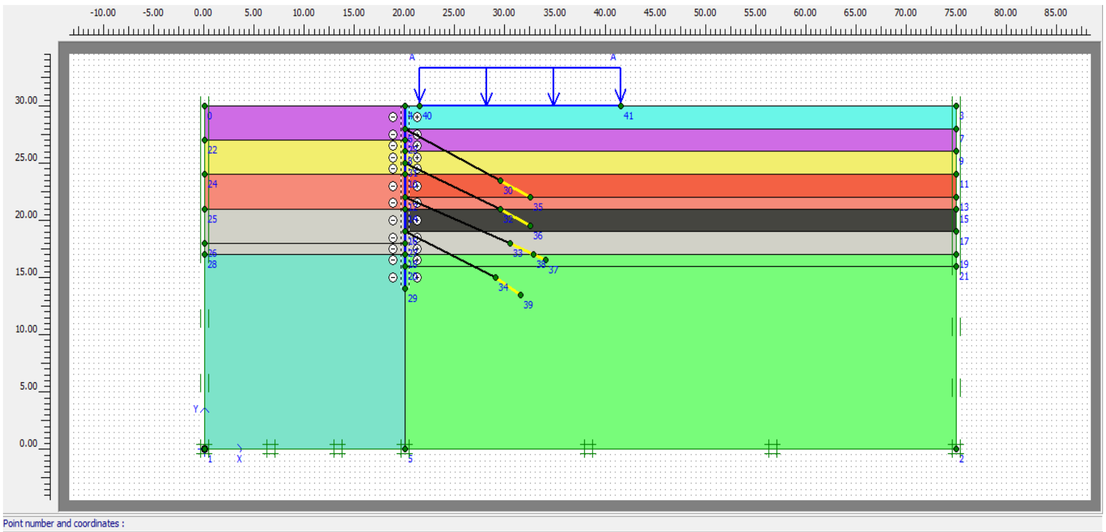

Figure 4-1: Finite element model used in PLAXIS for deep excavation

The relevant soil properties used for the base model, drained material model is used for silty-sand soil. In the simulations, soil elements were modeled with 15-node wedge elements that are generated from the projection of two-dimensional 6-node triangular elements between work planes with a width of 75 meters and depth of 30 meters.

The secant pile wall is modeled as elastic beam elements in which the unloading of the ground during the installation of secant pile wall is not considered. The Young's modulus, Es = 30000 Mpa, of the secant pile wall is kept constant for all the analyses, also with 60cm thickness of the secant pile wall. In addition to that, interface elements are also taken into consideration to model the soil-structure behavior.

The tieback anchors are installed into the secant pile wall. Each anchor is inclined at 24° with vertical spacing of 3m. The anchors assumed to have tensile strength, EA, of 1.00E+05 kN/m and pre-stressed load of 150 KN. At the end of tieback anchors, a geo-grid of 5m length is installed. Geo-grid, which has no bending stiffness but axial stiffness only, allows a continuous load transfer from the tieback anchors to the ground along its entire length. The tieback anchors were modeled with horizontal beams elements and the supporting walls were "wished into place," which means that the installation of the wall caused no stress changes or displacements in the surrounding soil. Excavations in silty sand soils with depth of 9m, 11m and 13m were considered in this study.

4.3 Parametric study and discussion

In this section a total of 18 parametric studies has done and a representative parametric study are presented. The parametric study conducted included the effects of surcharge location and increase in surcharge in horizontal displacement of the pile (δhmaxp), ground settlement behind the pile(δvmaxp) and bending moment of pile (Mmaxp) are presented and discussed for excavation depth of 9m, 11m and 13m including their construction stages.

The typical construction phases are summarized below.

Table 4-1: Typical construction phases for 9m excavation

	Initial phase
Phase 1	Pile and wall installation
Phase 2	Excavation to first level RL-4.00m
Phase 3	Installation of anchor at RL-3.00m
Phase 4	Excavation to second level RL-7.00m
Phase 5	Installation of anchor at RL-6.00m
Phase 6	Excavation to final level RL-9.00m

4.3.1 Effect of Change in surcharge

In this section the amount of surcharge is increased from 100kN/m^{2}to 120kN/m^2 and 140kN/m^{2}and are placed at a distance of 1.5m from edge of excavation and the horizontal displacement ratio, settlement ratio and bending moment ratio results behind the pile wall are presented and discussed. For analysis the soil, pile and anchor parameters listed from table 3.1 to table 3.5 are used.

4.3.1.1 Horizontal Displacement

The horizontal displacement ratio occurred in the pile for excavation depth of 9m, 11m and 13m are presented in the figure below.

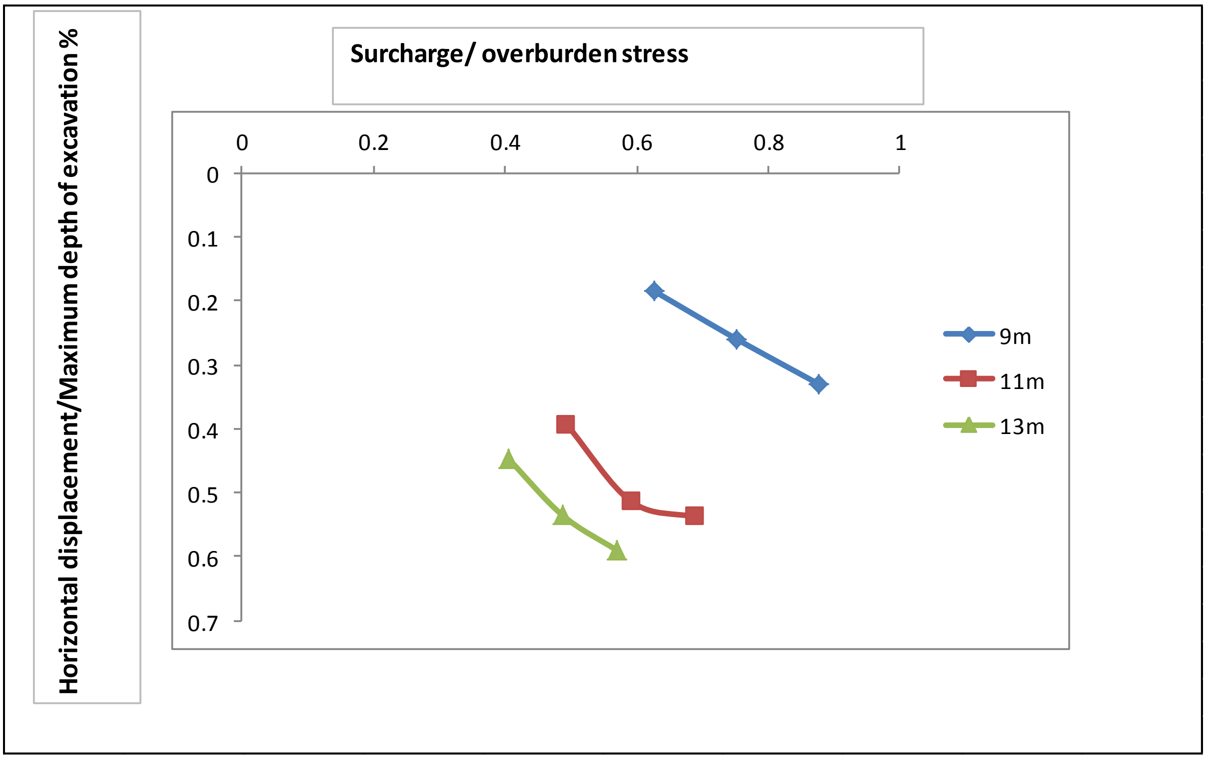

Figure 4-2: Horizontal displacement ratio behind the pile wall

The horizontal displacement ratio behind the pile wall increase as the ratio of surcharge to soil stress at bottom of excavation increases. Also it increases as the depth of excavation increases.

4.3.1.2 Vertical Displacement

The vertical displacement ratio occurred in the pile for excavation depth of 9m, 11m and 13m are presented in the figure below.

From the figure below as the ratio of surcharge to stress due to soil increases, the ratio of vertical displacement to maximum depth of excavation increase. Also it increases as the depth of excavation increases.

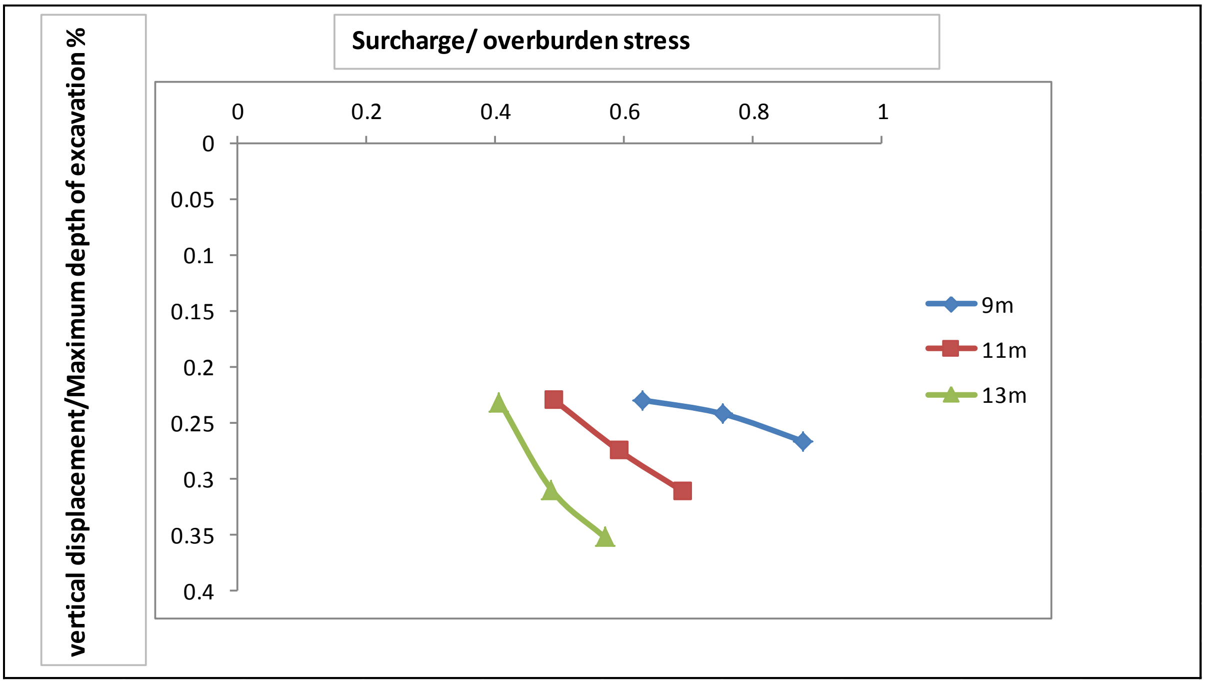

Figure 4-3: vertical displacement ratio behind the pile wall

4.3.1.3 Bending moment

This section deals with the bending moments occurred in the pile for excavation depth of 9m, 11mnand 13m. For analysis the soil, Pile and anchor parameters listed from table 3.1 to table 3.5 are used.

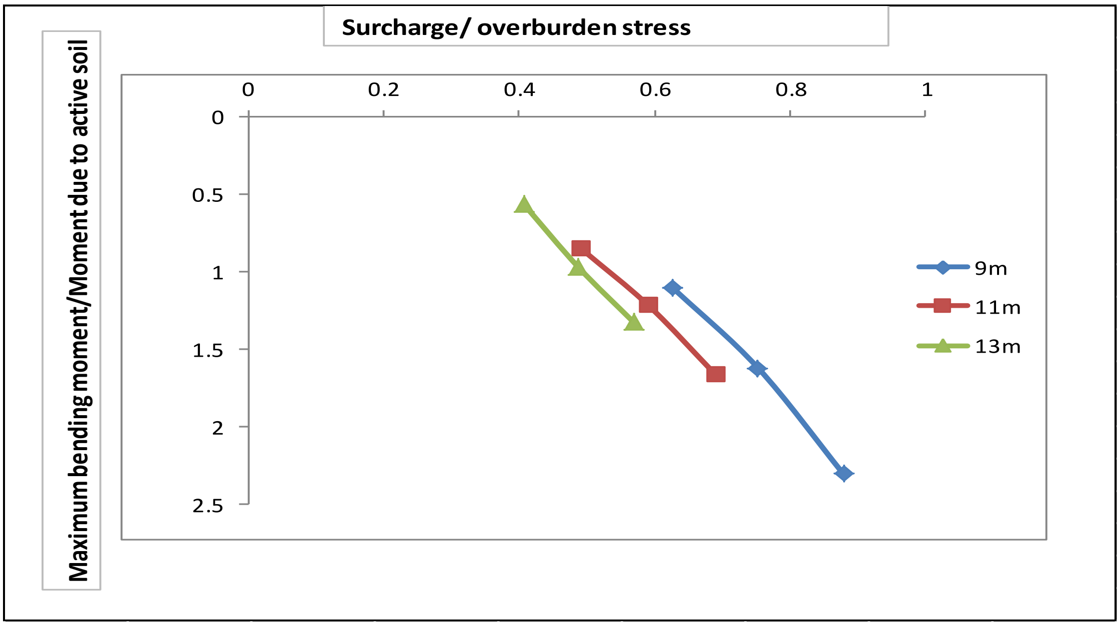

Figure 4-4: Bending moment behind the pile wall

The maximum bending moment to moment due to active soil mass ratio behind the pile wall increases as the surcharge to stress ratio at bottom of excavation increases. But it decreases as the depth of excavation increases.

4.3.2 Effect of Change in location of surcharge.

In this section, a surcharge of 100kN/m^{2}is placed at a distance of 1.5m, 5m, and 7.5m and the horizontal displacement ratio, settlement ratio and bending moment ratio results behind the pile wall are presented and discussed. For analysis the soil, pile and anchor parameters listed from table 3.1 to table 3.5 are used.

4.3.2.1 Horizontal Displacement

The horizontal displacement ratio occurred in the pile for excavation depth of 9m, 11m and 13m are presented in the figure below.

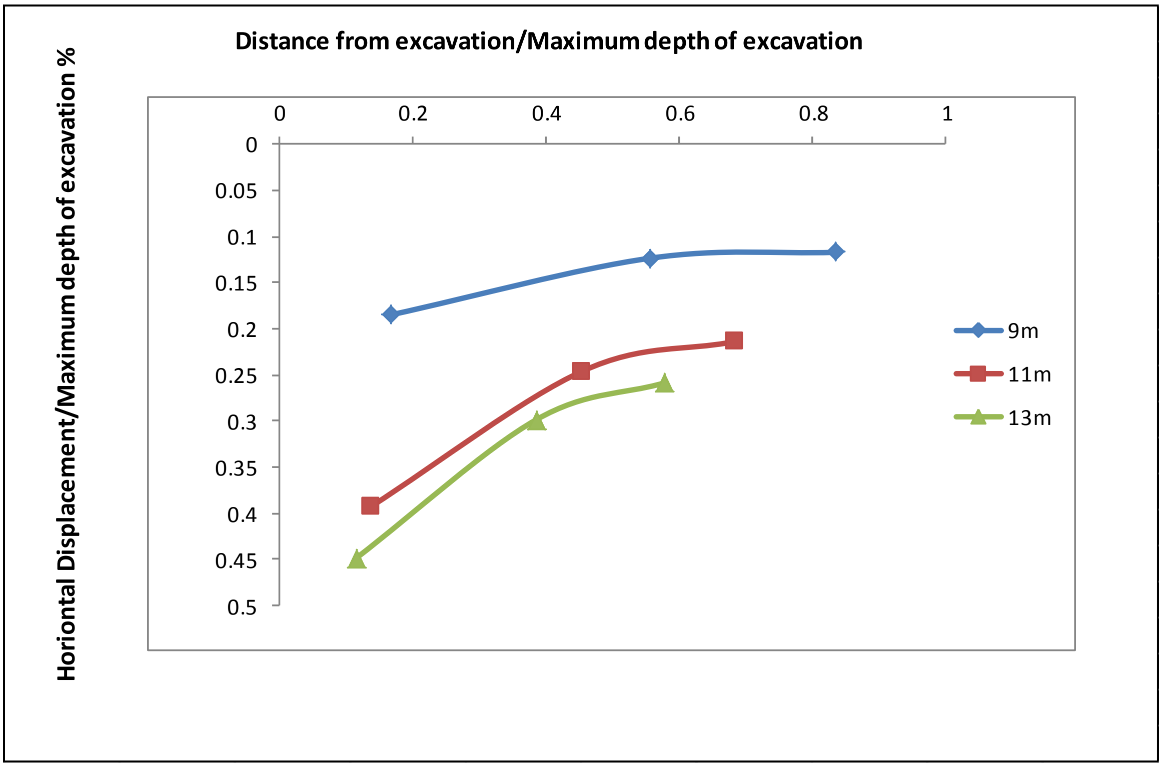

Figure 4-5: Horizontal displacement ratio behind the pile wall.

The ratio of horizontal displacement to maximum depth of excavation decreases as ratio of distance from excavation to maximum depth of excavation increases but increases as the depth of excavation increases.

4.3.2.2 Vertical Displacement.

The vertical displacement ratio occurred in the pile for excavation depth of 9m, 11m and 13m are presented in the figure below.

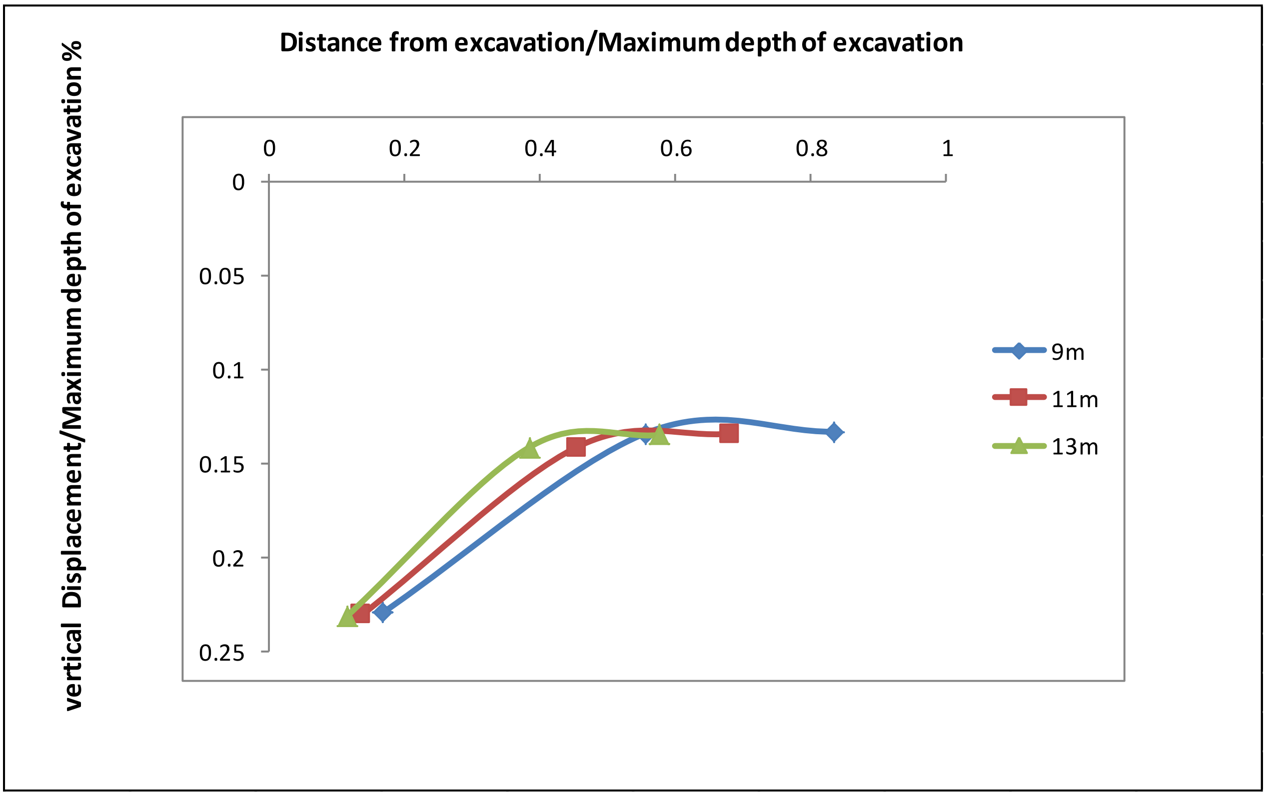

Figure 4-6: vertical displacement ratio behind the pile wall.

The ratio of vertical displacement to maximum depth of excavation decrease as the ratio of distance from excavation to maximum depth of excavation increases but increases as the depth of excavation increases.

4.3.2.3 Bending moment

This section deals with the bending moments occurred in the pile for excavation depth of 9m, 11m and 13m.From the figure below it can be concluded that the maximum bending moment to active soil moment ratio decrease as the location of surcharge is increased. Also decrease as the depth of excavation increases.

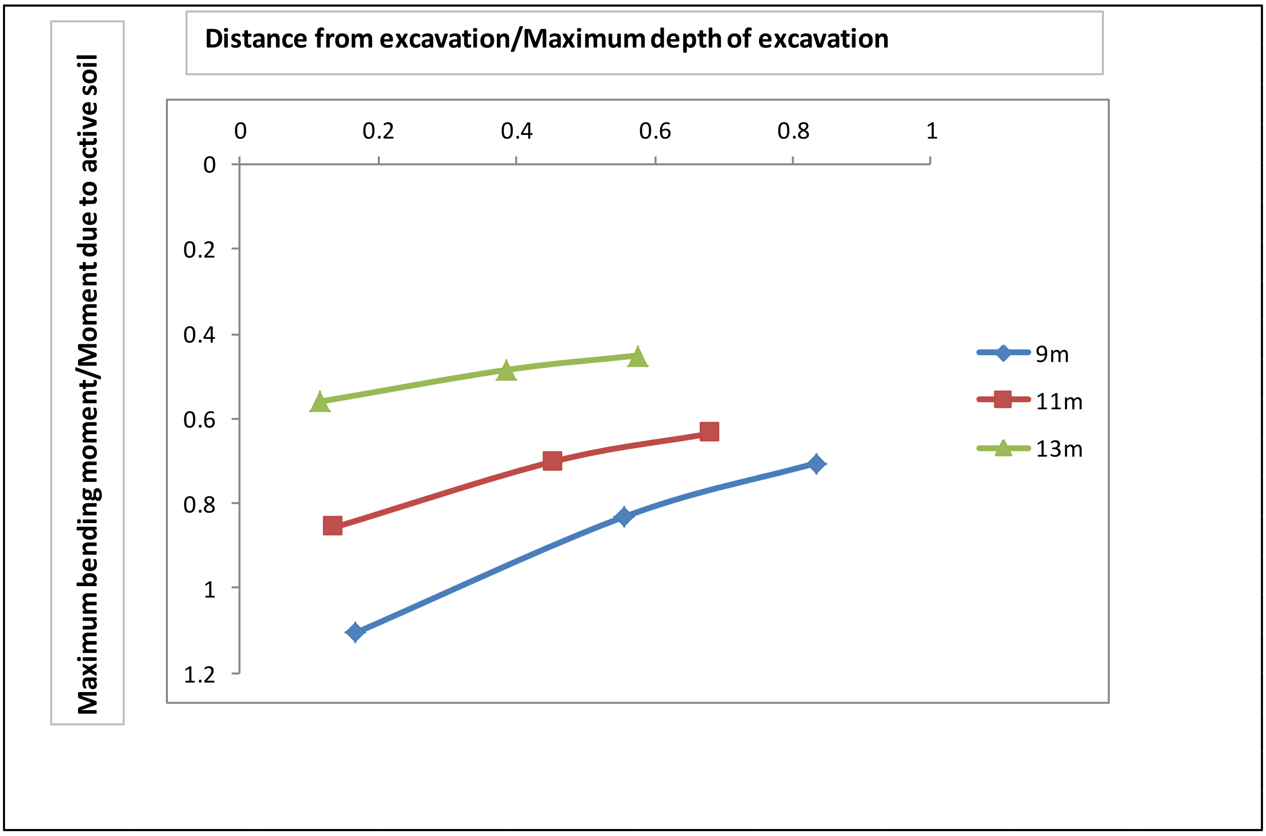

Figure 4-7: Bending moment behind the pile wall

CHAPTER FIVE: CONCLUSION AND RECOMMENDATION

5.1 Conclusion

This thesis is concerned with analysis of secant pile walls as deep excavation support system using PLAXIS 2D that is based on finite element analysis. Secant pile walls can be effectively used for deep excavation support to increase the bearing capacity, reduce ground movements, prevents sliding failure and control seepage by acting as retaining system.

Based on the study and results found during analysis the following conclusions can be withdrawn:

1. Since the performance of deep excavation support system and lateral wall movements are influenced by several factors including wall installation, soil conditions, support system stiffness, and methods of support system installation and interaction between the soil and the support, parameters have to be identified accordingly.
2. As the distance, increase from the depth of excavation for constant load the ratio of horizontal displacement to maximum depth of excavation decreases as ratio of distance from excavation to maximum depth of excavation increases but increases as the depth of excavation increases. However, for constant distance as the load increase the horizontal displacement ratio behind the pile wall increase as the ratio of surcharge to overburden stress of the soil increases. In addition, it increases as the depth of excavation increases.
3. For constant distance as the surcharge, increase the ratio of vertical displacement to maximum depth of excavation also increase. In addition, increase as the depth of excavation increases. For constant load as the distance increase the ratio of vertical displacement to maximum depth of excavation

decrease as the ratio of distance from excavation to maximum depth of excavation increases but increases as the depth of excavation increases.

4. The maximum bending moment to active moment of soil ratio decrease as the location of surcharge is increase. Also, decrease as the depth of excavation increases. The maximum bending moment to moment due to active soil mass ratio behind the pile wall increases as the surcharge to stress ratio at bottom of excavation increases. However, it decreases as the depth of excavation increases.
5. In the study of peck as the distance from excavation to the maximum depth of excavation increase the settlement to maximum depth of excavation tend to approach to zero but in this case the result tend to approach to none zero value.

5.2 Recommendations for future work

Deep excavation analysis requires a number of parameters, different issues have been addressed in this thesis, and various useful conclusions are drawn above. Nevertheless, there are still some unsolved problems worth further investigation.

- The surface load or surcharge is assumed as uniformly distributed. Analysis has not conducted for non-uniform load. This has to be considered for further study.
- The effect of change in anchor spacing, soil stiffness and wall embedment depth on horizontal and vertical displacement and bending moment behind the pile wall has not studied here. Hence, for future research one has to conduct a parametric study.
- It is very important to have an effective instrumentation and monitoring scheme to make sure that during excavation and construction of the basement, the safety of the surrounding properties can be secured. The instrumentation and monitoring scheme also allows the design engineer to validate the design and to identify the need to remedial measurements or alterations to the construction sequences before the serviceability of retaining

structure or the surrounding properties building and services are affected, its effective to do back-analysis based on the measurements. This can be considered for further study.

- Since PLAIXS 2D ignores the corner effects of excavation on deformation and bending moment, its effective to use PLAXIS 3D for further analysis.

APPENDIX I: THE HARDENING SOIL MODEL

The numerical modeling is going to be carried out by means of the finite-element method as it allows for modeling complicated nonlinear soil behavior and various interface conditions, with different geometries and soil properties.

PLAXIS program will be used, this program has a series of advantages:

- Excess pore pressure: Ability to deal with excess pore-pressure phenomena. Excess pore pressures are computed during plastic calculations in undrained soil.
- Soil-pile interaction: Interfaces can be used to simulate intensely shearing zone in contact with the pile, with values of friction angle and adhesion different to the friction angle and cohesion of the soil. Better insight into soil-structure interaction.
- Automatic load stepping: The program can run in an automatic step-size and an automatic time step selection mode, providing this way robust results.
- Dynamic analysis: Possibility to analyze vibrations and wave propagations in the soil.
- Soil model: It can reproduce advanced constitutive soil models for simulation of non-linear behavior.

Model election: soil, pile and interface

The available soil models are (PLAXIS Version 8):

1. Linear elastic model: it is the simplest available stress-strain relationship. According to the Hooke law, it only provides two input parameters, i.e. Young's modulus E and Poisson's ratio v. It is NOT suitable here because soil under load behaves strongly in elastically. However, this will be used to model the pile.

2. Mohr-Coulomb model: it is a perfectly elasto-plastic model of general scope, thus, has a fixed yield surface. It involves five input parameters, i.e. E and v for soil elasticity, the friction angle ϕ and the cohesion c for soil plasticity, and the angle of dilatancy ψ. It is a good first-order model, reliable to provide us with a trustful first insight into the problem.

Advantages:

For each layer one estimates a constant average stiffness. Due to this constant stiffness computations are quite fast and give a good first impression of the problem.

Shortcomings: It can be too simple

3. Jointed rock model: it is thought to model rock, NOT suitable here.
4. Hardening-soil model: it is an advanced hyperbolic soil model formulated in the framework of hardening plasticity. The main difference with the Mohr-Coulomb model is the stiffness approach. Here, the soil is described much more accurately by using three different input stiffness: triaxial loading stiffness E_{50}, triaxial unloading stiffness E_{ur} and the Oedometer loading stiffness E_{oed}. Apart from that, it accounts for stress-dependency of the stiffness moduli, all stiffness's increase with pressure (all three inputs relate to reference stress, 100kP a).

Advantages:

- More accurate stiffness definition than the Mohr-Coulomb model (stress-dependent and stress-path dependent stiffness).
- Takes into consideration soil dilatancy.
- The yield surface can expand due to plastic straining.

Shortcomings:

- Higher computational costs.
- Does not include viscous effects.

- Does not include softening.

5. Soft-soil-creep model: for soft soil (normally consolidated clays, silt or peat). NOT suitable here.
6. Soft soil model: for soft soil (normally consolidated clays, silt or peat). NOT suitable here.

For all the reasons presented above, **hardening soil model** is the most appropriate to model the soil.

Theoretical background

The Hardening Soil model has been presented before as a hyperbolic model. Often hyperbolic soil models have been used to describe the nonlinear behavior; this is also a suitable application in this research as silty-sand usually behaves as a linear elastic material with shear modulus G for shear strains up to ≈ 10−5, and afterward the stress-strain relationship is strongly non-linear (Lee, Salgado, 1999). The background of this kind of models is the hyperbolic relationship between vertical strain and deviatoric stress in primary triaxial loading. However, the Hardening-soil model is far better than the original hyperbolic model (Duncan and Chang, 1970) as it uses theory of plasticity instead of theory of elasticity and because it includes soil dilatancy and a yield cap. In contrast to an elastic perfectly-plastic model like Mohr-Coulomb, now the yield surface is not fixed but can expand due to plastic straining.

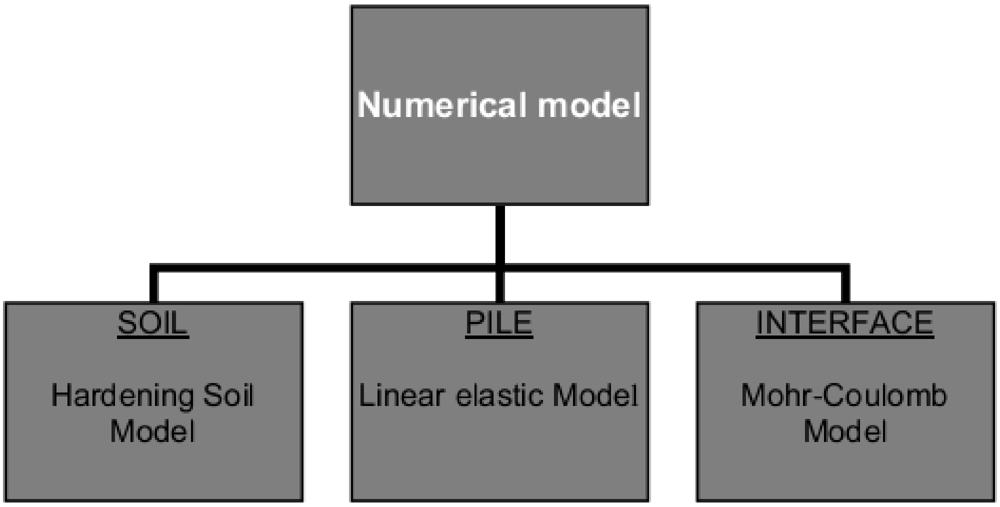

Figure 1. Chosen models for numerical analysis with PLAXIS

The main characteristics of the model are:

- Stress dependent stiffness according to power law (defined by parameter m).
- Plastic straining due to primary deviatoric stress (defined by parameter E_{50}^{ref}).
- Plastic straining due to primary compression (defined by parameter E_{oed}^{ref}).
- Elastic unloading/reloading (defined by parameter E_{ur}^{ref}, v_{ur}).
- Failure according to the Mohr-Coulomb model (defined by parameters c,ϕ,ψ)

In the Hardening Soil model, the associated flow rule is defined as a relationship between rates of plastic shear strain γ^p and plastic volumetric strain ξ_v^p; it has the linear form:

$$\epsilon_v^p = \sin\psi_m \gamma^p$$ Equation….1

Where: ψ_m is the mobilized dilatancy angle, defined as:

$$\sin\psi_m = \frac{\sin\varphi_m - \sin\varphi_{cv}}{1 - \sin\varphi_m \sin\varphi_{cv}}$$ Equation ……2

with ϕ_{cv} the critical state friction angle, constant for a certain material, independent of the density, and ϕ_m the mobilized friction angle that can be calculated:

$$\sin\varphi_m = \frac{\sigma_1^{'} - \sigma_3^{'}}{\sigma_1^{'} + \sigma_3^{'} - 2c\cos\varphi}$$

Equation…….3

According to Rowe's stress-dilatancy theory (1962), material contracts for small stress ratios ($\phi_m < \phi_{cv}$) and dilates for high stress-ratios ($\phi_m > \phi_{cv}$). At failure, the mobilized friction angle equals the failure one and:

$$\sin\psi = \frac{\sin\varphi - \sin\varphi_{cv}}{1 - \sin\varphi\sin\varphi_{cv}}$$

Equation….4

$$\sin\varphi_{cv} = \frac{\sin\varphi - \sin\psi}{1 - \sin\varphi\sin\psi}$$

Equation …5

The parameters of the model are those of Mohr-Coulomb for the failure criteria (c,ϕ,ψ); in addition other parameters are introduced

- Secant stiffness in standard drained triaxial test:E_{50}^{ref}, and then:

$$E_{50}(\sigma) = E_{50}^{ref}\left(\frac{c\cos\varphi - \sigma_3^{'}}{c\cos\varphi + p^{ref}\sin\varphi}\right)$$

Equation….6

- Tangent stiffness for primary Oedometer loading: E_{oed}^{ref}.
- Power for stress-level dependency of stiffness:m
- Unloading/reloading stiffness:E_{ur}^{ref} (default: $E_{ur}^{ref} = 3E_{50}^{ref}$), and then:

Equation….7

$$E_{ur}(\sigma) = E_{ur}^{ref}\left(\frac{c\cos\varphi - \sigma_3^{'}}{c\cos\varphi + p^{ref}\sin\varphi}\right)$$

- Poisson's ratio for unloading/reloading: ν_{ur} (default: ν_{ur}= 0.2).
- Reference stress for stiffness: p_{ref} (default: p_{ref}= 100 stress units).
- K_0 value for normal consolidation: K_o^{nc} (default: K_o^{nc}= 1 − sin ϕ).
- Failure ratio: Rf= q_f/q_a (default: R_f= 0.9).
- Tensile strength: $\sigma_{tension}$ (default: $\sigma_{tension}$ = 0).

Also it defines the Oedometer stiffness:

$$E_{oed} = E_{oed}^{ref}\left(\frac{c\cos\varphi - \sigma_1^{'}\sin\varphi}{c\cos\varphi + p^{ref}\sin\varphi}\right)^m$$ Equation….8

Note that the Oedometer stiffness relates to Oedometer testing, therefore to the compaction hardening part. On the other hand, $E_{50}$and E_{ur} relate to triaxial testing and so to the friction hardening part. To explain the plastic volumetric strain in isotropic compression, a second yield surface closes the elastic region in the direction of the p-axis. While the shear yield surface is mainly controlled by the triaxial modulus, the Oedometer modulus controls the cap yield surface.

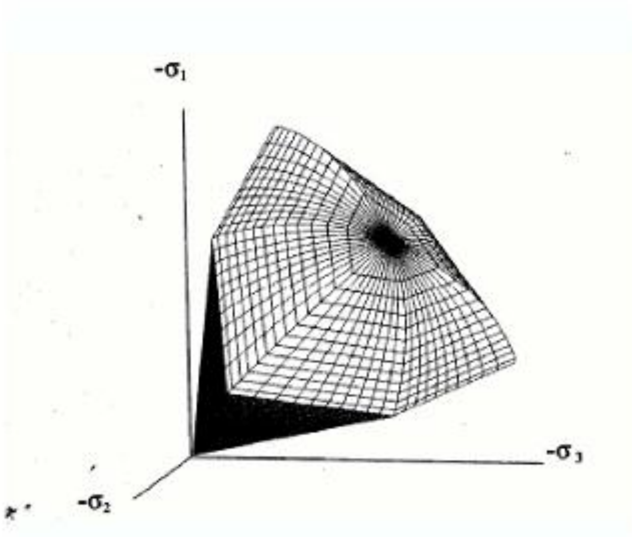

Figure 2. Cap surface of Hardening Soil model

APPENDIX II: ANCHOR LOAD AND EMBEDMENT DEPTH CALCULATION

For 9m excavation depth

For 100KN

no of anchor	2		H1	3	
spacing	3	3	H2	3	
locatin of upper anchor	3		H3	3	

Apparent earth pressure

Due to soil		Due to Surcharge qs=100KN/m2	
Pe=(0.65 *Ka*ᵞ*H^2)/(H-H1/3-Hn/3)		Ps=Ka*qs	qs= 100

H	9	m
ᵞ	17.71	KN/m3
ϕ1	36.32	
Ka1	0.232	
ᵞ	22	KN/m3
ϕ2	40	
Ka2	0.2	

Upper layer		lower layer	
α	90	α	90
β	0	β	0
δ	24.21333333	δ	26.66667

Pe	30.90344				
Ps	23.2				
pw	23.544	pw1	1.4715	pw2	17.1675

ANCHOR LOAD CALCULATION

T1=(2*H1/3+H2/2)*Pe + (H1+H2/2)*Ps	212.5621	KN
T2=(H2/2+23*H3/48)*Pe + (H2/2+H3/2)*Ps+pw	159.2017	KN
Rc= (3H3/16)*Pe + H3/2*Ps+pw	69.77987	KN

ANCHOR DESIGN LOAD CALCULATION

Assuming 20 degree inclination and c/c spacing 2.5 m

1. Upper anchor	565.3246
2. Lower anchor	423.4087

Design anchor load will be the largest which is 565.325 KN

Max. Anchor bond length		
8.697302	7.931939	3.565894
6.51398	5.94075	2.670732

For the existing soil condition the bond zone is formed in medium dense silt sand layer. Hence a load transfer of 130KN/m is selected assuming FS= 2 and 12m bond length

bondth strength= 130*BL/FS	780	>	565.3246	SAFE

DEPTH OF EMBEDEMENT CALCULATION

assuming wall as frictioal

δ1	24.21333333	β	0	ϕ1	36.32
δ2	26.66666667	α	90	ϕ2	40

Using coulomb's equation

Ka1	0.232	Kp	11.57
Ka2	0.2		

Earth pressure

Due to surcharge

q1	23.2	KN/m
q2	20	KN/m

Due to soil

		Depth	pressure	Force= F cos δ	moment arm	Moment
Active	Soil	0	0	0	0	0
		9	36.97848	151.7596819	3+D	455.28+151.76D
		(9+D)	31.878+4.4D	29.07D+2D^2	D/2 & D/3	14.53D^2+0.67D^3
	Surcharge	0	23.2	0	0	0
		9	23.2	190.4256	4.5+D	856.92+190.43D
		9+D	20	18.24D	0.5D	9.12D^2
Passive	Soil	0	0	0	0	0
		D	254.5D	116.1D^2	D/3	38.69D^3
	Strut 1		212.562054	212.562054	6+D	1275.4+212.56D
	strut 2		159.2016668	159.2016668	3+D	477.6+159.2D
	Reaction		69.77987475	69.77987475	D	69.78D

Assuming FS against overturning as 1.5, using trial and error

D=2.8m

Increasing by 20%

D=4m

For 120KN

no of anchor	2		H1 3
spacing	3	3	H2 3
locatin of upper anchor	3		H3 3

Apparent earth pressure

Due to soil	Due to Surcharge qs=120KN/m2
Pe=(0.65 *Ka*ᵞ*H^2)/(H-H1/3-Hn/3)	Ps=Ka*qs qs= 120

H	9	m
ᵞ	17.71	KN/m3
ϕ1	36.32	
Ka1	0.232	
ᵞ	22	KN/m3
ϕ2	40	
Ka2	0.2	

Upper layer		lower layer	
α	90	α	90
β	0	β	0
δ	24.21333333	δ	26.66667

Pe	30.90344				
Ps	27.84				
pw	18.639	pw1	1.4715	pw2	17.1675

ANCHOR LOAD CALCULATION

T1=(2*H1/3+H2/2)*Pe + (H1+H2/2)*Ps	233.4421	KN
T2=(H2/2+23*H3/48)*Pe + (H2/2+H3/2)*Ps+pw	173.3669	KN
Rc= (3H3/16)*Pe + H3/2*Ps+pw	76.73987	KN

ANCHOR DESIGN LOAD CALCULATION

Assuming 20 degree inclination and c/c spacing 2.5 m

1. Upper anchor	620.8565
2. Lower anchor	461.0822

Design anchor load will be the largest which is 620.86KN

Max. Anchor bond length		
9.551639	8.711095	3.916172
7.093573	6.469338	2.908365

For the existing soil condition the bond zone is formed in medium dense silt sand layer. Hence a load transfer of 130KN/m is selected assuming FS= 2 and 12m bond length

bondth strength= 130*BL/FS	780	>	620.8565	SAFE

DEPTH OF EMBEDEMENT CALCULATION

assuming wall as frictioal

δ1	24.21333333	β	0	ϕ1	36.32
δ2	26.66666667	α	90	ϕ2	40

Using coulomb's equation

Ka1	0.232	Kp	11.57
Ka2	0.2		

Earth pressure

Due to surcharge

q1	27.84	KN/m
q2	24	KN/m

Due to soil

		Depth	pressure	Force= F cos δ	moment arm	Moment
Active	Soil	0	0	0	0	0
		9	36.97848	151.7596819	3+D	455.28+151.76D
		(9+D)	31.878+4.4D	29.07D+2D^2	D/2 & D/3	14.53D^2+0.67D^3
	Surcharge	0	27.84	0	0	0
		9	27.84	228.51072	4.5+D	1028.3+228.51D
		9+D	24	21.88D	0.5D	10.944D^2
Passive	Soil	0	0	0	0	0
		D	254.5D	116.1D^2	D/3	38.69D^3
	Strut 1		233.442054	233.442054	6+D	1400.65+233.442D
	strut 2		173.3669168	173.3669168	3+D	519.365+173.12D
	Reaction		76.73987475	76.73987475	D	76.74D

Assuming FS against overturning as 1.5, using trial and error

D=2.8m

Increasing by 20%

D=4m

For 140KN

no of anchor	2			H1	3
spacing	3	3		H2	3
locatin of upper anchor	3			H3	3

Apparent earth pressure

Due to soil

Pe=(0.65 *Ka*ᵞ*H^2)/(H-H1/3-Hn/3)

Due to Surcharge qs=140KN/m2

Ps=Ka*qs qs= 140

H	9	m
ᵞ	17.71	KN/m3
ϕ1	36.32	
Ka1	0.232	
ᵞ	22	KN/m3
ϕ2	40	
Ka2	0.2	

Upper layer		lower layer	
α	90	α	90
β	0	β	0
δ	24.21333	δ	26.66667

Pe	30.90344				
Ps	32.48				
pw	23.544	pw1	1.4715	pw2	17.1675

ANCHOR LOAD CALCULATION

T1=(2*H1/3+H2/2)*Pe + (H1+H2/2)*Ps	254.3221	KN
T2=(H2/2+23*H3/48)*Pe + (H2/2+H3/2)*Ps	187.0417	KN
Rc= (3H3/16)*Pe + H3/2*Ps+pw	83.69987	KN

ANCHOR DESIGN LOAD CALCULATION

Assuming 20 degree inclination and c/c spacing 2.5 m

1. Upper anchor	676.3884
2. Lower anchor	497.4512

Design anchor load will be the largest which is 676.4KN

Max. Anchor bond length			geo grid		
10.40598	9.49025	4.26645	4	3.648	1.64
7.653096	6.979624	3.137769	4	3.648	1.64

For the existing soil condition the bond zone is formed in medium dense silt sand layer. Hence a load transfer of 130KN/m is selected assuming FS= 2 and 12m bond length

bondth strength= 130*BL/FS 780 > 676.3884 SAFE

DEPTH OF EMBEDEMENT CALCULATION

assuming wall as frictioal

δ1	24.21333	β	0	ϕ1	36.32
δ2	26.66667	α	90	ϕ2	40

Using coulomb's equation

Ka1	0.232	Kp	11.57
Ka2	0.2		

Earth pressure

Due to surcharge

q1	32.48	KN/m
q2	28	KN/m

Due to soil

		Depth	pressure	Force= F c	moment arm	Moment
Active	Soil	0	0	0	0	0
		9	36.97848	151.7597	3+D	455.28+151.76D
		(9+D)	1.878+4.4	9.07D+2D^	D/2 & D/3	14.53D^2+0.67D^3
	Surcharge	0	32.48	0	0	0
		9	32.48	266.5958	4.5+D	1199.7+266.6D
		9+D	28	25.54D	0.5D	12.77D^2
Passive	Soil	0	0	0	0	0
		D	254.5D	116.1D^2	D/3	38.69D^3
	Strut 1		254.3221	254.3221	6+D	1525.9+254.32D
	strut 2		187.0417	187.0417	3+D	561.1+187D
	Reaction		83.69987	83.69987	D	83.7D

Assuming FS against overturning as 1.5, using trial and error

D=3m

Increasing by 20%

D=4m

APPENDIX III: PLAXIS OUTPUT

A) For 9m excavation @1.5m distance from excavation

x=1.5m	100kpa		120kpa		140kpa	
Y	Ux	Uy	Ux	Uy	Ux	Uy
[m]	[m]	[m]	[m]	[m]	[m]	[m]
30	-0.03947	-0.00561	-0.04217	-0.00679	-0.07067	-0.00811
29.75	-0.03876	-0.00561	-0.04189	-0.00679	-0.06967	-0.00811
29.5	-0.03805	-0.00561	-0.04161	-0.00679	-0.06868	-0.00811
29.25	-0.03734	-0.00561	-0.04133	-0.00679	-0.06767	-0.00811
29	-0.03661	-0.00561	-0.04103	-0.00679	-0.06666	-0.00811
29	-0.03661	-0.00561	-0.04103	-0.00679	-0.06666	-0.00811
28.75	-0.03588	-0.00561	-0.04072	-0.00679	-0.06563	-0.00811
28.5	-0.03513	-0.0056	-0.0404	-0.00679	-0.06459	-0.00811
28.25	-0.03439	-0.0056	-0.04008	-0.00679	-0.06354	-0.00811
28	-0.03365	-0.0056	-0.03975	-0.00678	-0.0625	-0.00811
28	-0.03365	-0.0056	-0.03975	-0.00678	-0.0625	-0.00811
27.75	-0.03296	-0.0056	-0.03946	-0.00678	-0.0615	-0.0081
27.5	-0.03228	-0.0056	-0.03917	-0.00678	-0.06051	-0.0081
27.25	-0.03162	-0.00559	-0.03887	-0.00677	-0.05951	-0.00809
27	-0.03095	-0.00559	-0.03855	-0.00677	-0.05849	-0.00809
27	-0.03095	-0.00559	-0.03855	-0.00677	-0.05849	-0.00809
26.75	-0.03029	-0.00558	-0.03819	-0.00676	-0.05745	-0.00808
26.5	-0.02964	-0.00558	-0.0378	-0.00676	-0.05638	-0.00808
26.25	-0.02898	-0.00557	-0.03736	-0.00675	-0.05528	-0.00807
26	-0.02833	-0.00557	-0.03688	-0.00674	-0.05416	-0.00806
26	-0.02833	-0.00557	-0.03688	-0.00674	-0.05416	-0.00806
25.75	-0.02769	-0.00556	-0.03636	-0.00674	-0.053	-0.00806

25.5	-0.02705	-0.00555	-0.03581	-0.00673	-0.05182	-0.00805
25.25	-0.02642	-0.00555	-0.03523	-0.00672	-0.05062	-0.00804
25	-0.02583	-0.00554	-0.03463	-0.00671	-0.04943	-0.00803
25	-0.02583	-0.00554	-0.03463	-0.00671	-0.04943	-0.00803
24.75	-0.02528	-0.00553	-0.03406	-0.0067	-0.04826	-0.00802
24.5	-0.02477	-0.00552	-0.03348	-0.00669	-0.0471	-0.00801
24.25	-0.02427	-0.00551	-0.03288	-0.00668	-0.04594	-0.008
24	-0.02377	-0.0055	-0.03226	-0.00667	-0.04476	-0.00798
24	-0.02377	-0.0055	-0.03226	-0.00667	-0.04476	-0.00798
23.75	-0.02328	-0.00549	-0.03161	-0.00666	-0.04356	-0.00797
23.5	-0.02279	-0.00548	-0.03093	-0.00665	-0.04234	-0.00796
23.25	-0.02228	-0.00547	-0.03021	-0.00663	-0.04109	-0.00795
23	-0.02176	-0.00546	-0.02945	-0.00662	-0.03981	-0.00793
23	-0.02176	-0.00546	-0.02945	-0.00662	-0.03981	-0.00793
22.75	-0.02123	-0.00544	-0.02866	-0.00661	-0.03851	-0.00792
22.5	-0.02069	-0.00543	-0.02783	-0.00659	-0.03719	-0.0079
22.25	-0.02015	-0.00542	-0.02699	-0.00658	-0.03586	-0.00789
22	-0.01962	-0.00541	-0.02616	-0.00656	-0.03454	-0.00787
22	-0.01962	-0.00541	-0.02616	-0.00656	-0.03454	-0.00787
21.75	-0.01913	-0.00539	-0.02535	-0.00655	-0.03327	-0.00785
21.5	-0.01866	-0.00537	-0.02456	-0.00653	-0.03202	-0.00783
21.25	-0.0182	-0.00536	-0.02378	-0.00651	-0.0308	-0.00782
21	-0.01773	-0.00534	-0.023	-0.0065	-0.02959	-0.0078
21	-0.01773	-0.00534	-0.023	-0.0065	-0.02959	-0.0078
20.75	-0.01726	-0.00533	-0.02222	-0.00648	-0.0284	-0.00778
20.5	-0.01677	-0.00531	-0.02143	-0.00646	-0.02722	-0.00776
20.25	-0.01627	-0.00529	-0.02064	-0.00644	-0.02605	-0.00774
20	-0.01574	-0.00528	-0.01983	-0.00642	-0.02488	-0.00771
20	-0.01574	-0.00528	-0.01983	-0.00642	-0.02488	-0.00771
19.75	-0.0152	-0.00526	-0.019	-0.0064	-0.0237	-0.00769

19.5	-0.01463	-0.00524	-0.01816	-0.00638	-0.02252	-0.00767
19.25	-0.01405	-0.00522	-0.01731	-0.00636	-0.02135	-0.00765
19	-0.01346	-0.0052	-0.01646	-0.00634	-0.02018	-0.00763
19	-0.01346	-0.0052	-0.01646	-0.00634	-0.02018	-0.00763
18.75	-0.01289	-0.00518	-0.01565	-0.00632	-0.01905	-0.0076
18.5	-0.01233	-0.00516	-0.01484	-0.00629	-0.01794	-0.00758
18.25	-0.01176	-0.00514	-0.01403	-0.00627	-0.01684	-0.00755
18	-0.01118	-0.00512	-0.01322	-0.00625	-0.01575	-0.00753
18	-0.01118	-0.00512	-0.01322	-0.00625	-0.01575	-0.00753
17.75	-0.01059	-0.0051	-0.01241	-0.00622	-0.01467	-0.0075
17.5	-0.00999	-0.00508	-0.01161	-0.0062	-0.01362	-0.00747
17.25	-0.00941	-0.00506	-0.01084	-0.00617	-0.01261	-0.00745
17	-0.00885	-0.00503	-0.01011	-0.00615	-0.01166	-0.00742
17	-0.00885	-0.00503	-0.01011	-0.00615	-0.01166	-0.00742
16.75	-0.00836	-0.00501	-0.00946	-0.00613	-0.01081	-0.00739
16.5	-0.00796	-0.00499	-0.00892	-0.0061	-0.01009	-0.00737
16.25	-0.00763	-0.00498	-0.00848	-0.00608	-0.0095	-0.00735
16	-0.00737	-0.00496	-0.00813	-0.00606	-0.00903	-0.00733
16	-0.00737	-0.00496	-0.00813	-0.00606	-0.00903	-0.00733
15.75	-0.00717	-0.00494	-0.00785	-0.00604	-0.00865	-0.00731
15.5	-0.00702	-0.00493	-0.00763	-0.00603	-0.00834	-0.00729
15.25	-0.00689	-0.00491	-0.00745	-0.00601	-0.0081	-0.00727
15	-0.00679	-0.0049	-0.00731	-0.006	-0.0079	-0.00725
15	-0.00679	-0.0049	-0.00731	-0.006	-0.0079	-0.00725
14.75	-0.0067	-0.00489	-0.00718	-0.00598	-0.00773	-0.00724
14.5	-0.00662	-0.00488	-0.00707	-0.00597	-0.00757	-0.00723
14.25	-0.00654	-0.00487	-0.00696	-0.00596	-0.00742	-0.00722
14	-0.00646	-0.00486	-0.00685	-0.00595	-0.00728	-0.0072

For 5m distance from the excavation

x=5m	100kpa		120kpa		140kpa	
Y	Ux	Uy	Ux	Uy	Ux	Uy
[m]	[m]	[m]	[m]	[m]	[m]	[m]
30	-0.03897	-0.00561	-0.01089	0.000493	-0.01493	0.000575
29.75	-0.03876	-0.00561	-0.01099	0.000493	-0.01506	0.000575
29.5	-0.03805	-0.00561	-0.01108	0.000493	-0.01518	0.000576
29.25	-0.03744	-0.00561	-0.01118	0.000493	-0.0153	0.000576
29	-0.03661	-0.00561	-0.01127	0.000494	-0.01542	0.000576
29	-0.03661	-0.00561	-0.01127	0.000494	-0.01542	0.000576
28.75	-0.03588	-0.00561	-0.01135	0.000494	-0.01552	0.000577
28.5	-0.03523	-0.0056	-0.01143	0.000494	-0.01562	0.000577
28.25	-0.03439	-0.0056	-0.0115	0.000495	-0.01571	0.000578
28	-0.03365	-0.0056	-0.01155	0.000495	-0.01578	0.000579
28	-0.03365	-0.0056	-0.01155	0.000495	-0.01578	0.000579
27.725	-0.03296	-0.0056	-0.0116	0.000496	-0.01584	0.000579
27.45	-0.03228	-0.0056	-0.01164	0.000497	-0.01588	0.00058
27.175	-0.03162	-0.00559	-0.01167	0.000497	-0.01592	0.000582
26.9	-0.03095	-0.00559	-0.01171	0.000498	-0.01596	0.000583
26.9	-0.03095	-0.00559	-0.01171	0.000498	-0.01596	0.000583
26.675	-0.03029	-0.00558	-0.01176	0.000501	-0.01602	0.000586
26.45	-0.02964	-0.00558	-0.01182	0.000503	-0.01607	0.000589
26.225	-0.02898	-0.00557	-0.01188	0.000506	-0.01612	0.000592
26	-0.02833	-0.00557	-0.01191	0.000509	-0.01615	0.000596
26	-0.02833	-0.00557	-0.01191	0.000509	-0.01615	0.000596
25.75	-0.02769	-0.00556	-0.01192	0.000512	-0.01616	0.0006
25.5	-0.02705	-0.00555	-0.0119	0.000516	-0.01613	0.000604

25.25	-0.02642	-0.00555	-0.01184	0.000519	-0.01605	0.000609
25	-0.02583	-0.00554	-0.01173	0.000523	-0.01592	0.000613
25	-0.02583	-0.00554	-0.01173	0.000523	-0.01592	0.000613
24.75	-0.02528	-0.00553	-0.01159	0.000527	-0.01574	0.000618
24.5	-0.02477	-0.00552	-0.0114	0.000531	-0.01549	0.000623
24.25	-0.02427	-0.00551	-0.01118	0.000535	-0.01518	0.000628
24	-0.02377	-0.0055	-0.01093	0.00054	-0.01479	0.000634
24	-0.02377	-0.0055	-0.01093	0.00054	-0.01479	0.000634
23.7	-0.02328	-0.00549	-0.01063	0.000548	-0.01425	0.000641
23.4	-0.02279	-0.00548	-0.0103	0.000556	-0.01361	0.000649
23.1	-0.02228	-0.00547	-0.00993	0.000564	-0.0129	0.000657
22.8	-0.02176	-0.00546	-0.00952	0.000573	-0.01214	0.000666
22.8	-0.02176	-0.00546	-0.00952	0.000573	-0.01214	0.000666
22.6	-0.02123	-0.00544	-0.00924	0.000579	-0.01163	0.000672
22.4	-0.02069	-0.00543	-0.00897	0.000584	-0.01113	0.000677
22.2	-0.02015	-0.00542	-0.0087	0.00059	-0.01066	0.000683
22	-0.01962	-0.00541	-0.00844	0.000595	-0.0102	0.000688
22	-0.01962	-0.00541	-0.00844	0.000595	-0.0102	0.000688
21.75	-0.01913	-0.00539	-0.00813	0.000602	-0.00968	0.000695
21.5	-0.01866	-0.00537	-0.00786	0.000608	-0.00921	0.000701
21.25	-0.0182	-0.00536	-0.0076	0.000614	-0.0088	0.000707
21	-0.01773	-0.00534	-0.00738	0.00062	-0.00843	0.000713
21	-0.01773	-0.00534	-0.00738	0.00062	-0.00843	0.000713
20.75	-0.01726	-0.00533	-0.00719	0.000625	-0.00813	0.000719
20.5	-0.01677	-0.00531	-0.00703	0.00063	-0.00788	0.000724
20.25	-0.01627	-0.00529	-0.0069	0.000635	-0.00767	0.000729
20	-0.01574	-0.00528	-0.00678	0.000639	-0.0075	0.000733
20	-0.01574	-0.00528	-0.00678	0.000639	-0.0075	0.000733
19.75	-0.0152	-0.00526	-0.00669	0.000643	-0.00735	0.000737
19.5	-0.01463	-0.00524	-0.00661	0.000646	-0.00723	0.000741

19.25	-0.01405	-0.00522	-0.00653	0.000649	-0.00713	0.000744
19	-0.01346	-0.0052	-0.00647	0.000652	-0.00704	0.000747
19	-0.01346	-0.0052	-0.00647	0.000652	-0.00704	0.000747
18.75	-0.01289	-0.00518	-0.0064	0.000655	-0.00696	0.00075
18.5	-0.01233	-0.00516	-0.00635	0.000657	-0.00688	0.000753
18.25	-0.01176	-0.00514	-0.00629	0.000659	-0.00681	0.000755
18	-0.01118	-0.00512	-0.00624	0.000661	-0.00674	0.000757
18	-0.01118	-0.00512	-0.00624	0.000661	-0.00674	0.000757
17.75	-0.01059	-0.0051	-0.00618	0.000663	-0.00667	0.000759
17.5	-0.00999	-0.00508	-0.00613	0.000665	-0.0066	0.00076
17.25	-0.00941	-0.00506	-0.00608	0.000666	-0.00654	0.000762
17	-0.00886	-0.00504	-0.00603	0.000668	-0.00647	0.000763

For 11m excavation @5m distance from excavation

	100kpa		120kpa		140kpa	
Y	Ux	Uy	Ux	Uy	Ux	Uy
[m]	[m]	[m]	[m]	[m]	[m]	[m]
30	-0.01398	-0.00188	-0.01926	-0.00224	-0.02985	-0.00304
29.75	-0.014	-0.00188	-0.01922	-0.00224	-0.02972	-0.00304
29.5	-0.01401	-0.00188	-0.01917	-0.00224	-0.02959	-0.00304
29.25	-0.01402	-0.00188	-0.01912	-0.00224	-0.02946	-0.00304
29	-0.01403	-0.00188	-0.01907	-0.00224	-0.02933	-0.00304
29	-0.01403	-0.00188	-0.01907	-0.00224	-0.02933	-0.00304
28.75	-0.01405	-0.00188	-0.01903	-0.00224	-0.02919	-0.00304
28.5	-0.01407	-0.00188	-0.01898	-0.00224	-0.02906	-0.00304
28.25	-0.0141	-0.00188	-0.01894	-0.00223	-0.02893	-0.00304
28	-0.01416	-0.00188	-0.01893	-0.00223	-0.02882	-0.00304

28	-0.01416	-0.00188	-0.01893	-0.00223	-0.02882	-0.00304
27.75	-0.01426	-0.00188	-0.01895	-0.00223	-0.02874	-0.00304
27.5	-0.01437	-0.00188	-0.01899	-0.00223	-0.02868	-0.00303
27.25	-0.01448	-0.00187	-0.01902	-0.00223	-0.02861	-0.00303
27	-0.01458	-0.00187	-0.01904	-0.00222	-0.02853	-0.00303
27	-0.01458	-0.00187	-0.01904	-0.00222	-0.02853	-0.00303
26.75	-0.01467	-0.00187	-0.01905	-0.00222	-0.02843	-0.00303
26.5	-0.01474	-0.00186	-0.01903	-0.00222	-0.0283	-0.00302
26.25	-0.01478	-0.00186	-0.019	-0.00221	-0.02814	-0.00302
26	-0.0148	-0.00186	-0.01893	-0.00221	-0.02796	-0.00302
26	-0.0148	-0.00186	-0.01893	-0.00221	-0.02796	-0.00302
25.75	-0.01479	-0.00186	-0.01885	-0.00221	-0.02775	-0.00301
25.5	-0.01477	-0.00185	-0.01875	-0.0022	-0.02752	-0.00301
25.25	-0.01473	-0.00185	-0.01864	-0.0022	-0.02727	-0.003
25	-0.0147	-0.00184	-0.01853	-0.0022	-0.027	-0.003
25	-0.0147	-0.00184	-0.01853	-0.0022	-0.027	-0.003
24.75	-0.01469	-0.00184	-0.01844	-0.00219	-0.02675	-0.00299
24.5	-0.01468	-0.00183	-0.01835	-0.00218	-0.02649	-0.00299
24.25	-0.01465	-0.00183	-0.01825	-0.00218	-0.02619	-0.00298
24	-0.01461	-0.00182	-0.01813	-0.00217	-0.02586	-0.00297
24	-0.01461	-0.00182	-0.01813	-0.00217	-0.02586	-0.00297
23.75	-0.01453	-0.00181	-0.01797	-0.00216	-0.02549	-0.00297
23.5	-0.01443	-0.00181	-0.01777	-0.00216	-0.02506	-0.00296
23.25	-0.01428	-0.0018	-0.01754	-0.00215	-0.02458	-0.00295
23	-0.0141	-0.00179	-0.01727	-0.00214	-0.02405	-0.00294
23	-0.0141	-0.00179	-0.01727	-0.00214	-0.02405	-0.00294
22.75	-0.01389	-0.00178	-0.01695	-0.00213	-0.02347	-0.00293
22.5	-0.01364	-0.00178	-0.0166	-0.00212	-0.02283	-0.00293
22.25	-0.01338	-0.00177	-0.01623	-0.00212	-0.02215	-0.00292
22	-0.0131	-0.00176	-0.01584	-0.00211	-0.02144	-0.00291

22	-0.0131	-0.00176	-0.01584	-0.00211	-0.02144	-0.00291
21.75	-0.01284	-0.00175	-0.01546	-0.00209	-0.02074	-0.00289
21.5	-0.01257	-0.00174	-0.01507	-0.00208	-0.02002	-0.00288
21.25	-0.01229	-0.00173	-0.01467	-0.00207	-0.01928	-0.00287
21	-0.01199	-0.00172	-0.01424	-0.00206	-0.01852	-0.00286
21	-0.01199	-0.00172	-0.01424	-0.00206	-0.01852	-0.00286
20.75	-0.01167	-0.00171	-0.01379	-0.00205	-0.01773	-0.00284
20.5	-0.01131	-0.00169	-0.0133	-0.00203	-0.01692	-0.00283
20.25	-0.01092	-0.00168	-0.01278	-0.00202	-0.01608	-0.00282
20	-0.01051	-0.00167	-0.01222	-0.00201	-0.01522	-0.0028
20	-0.01051	-0.00167	-0.01222	-0.00201	-0.01522	-0.0028
19.75	-0.01006	-0.00166	-0.01164	-0.002	-0.01434	-0.00279
19.5	-0.0096	-0.00165	-0.01105	-0.00198	-0.01346	-0.00277
19.25	-0.00913	-0.00163	-0.01044	-0.00197	-0.01259	-0.00276
19	-0.00868	-0.00162	-0.00986	-0.00195	-0.01176	-0.00274
19	-0.00868	-0.00162	-0.00986	-0.00195	-0.01176	-0.00274
18.75	-0.00826	-0.00161	-0.00933	-0.00194	-0.011	-0.00272
18.5	-0.00791	-0.0016	-0.00888	-0.00193	-0.01034	-0.00271
18.25	-0.00762	-0.00159	-0.0085	-0.00192	-0.00978	-0.0027
18	-0.00739	-0.00158	-0.0082	-0.0019	-0.00932	-0.00269
18	-0.00739	-0.00158	-0.0082	-0.0019	-0.00932	-0.00269
17.75	-0.00721	-0.00157	-0.00795	-0.00189	-0.00895	-0.00268
17.5	-0.00706	-0.00156	-0.00776	-0.00189	-0.00865	-0.00266
17.25	-0.00695	-0.00155	-0.0076	-0.00188	-0.0084	-0.00266
17	-0.00686	-0.00154	-0.00747	-0.00187	-0.0082	-0.00265
17	-0.00686	-0.00154	-0.00747	-0.00187	-0.0082	-0.00265
16.75	-0.00678	-0.00154	-0.00736	-0.00186	-0.00803	-0.00264
16.5	-0.00671	-0.00153	-0.00726	-0.00186	-0.00787	-0.00263
16.25	-0.00664	-0.00153	-0.00717	-0.00185	-0.00773	-0.00263
16	-0.00657	-0.00152	-0.00708	-0.00185	-0.00758	-0.00262

For 11m excavation @ 7.5m distance from excavation

	100kpa		120kpa		140kpa	
Y	Ux	Uy	Ux	Uy	Ux	Uy
[m]	[m]	[m]	[m]	[m]	[m]	[m]
30	-0.01126	-0.00059	-0.01524	-0.00088	-0.01946	-0.001
29.75	-0.01127	-0.00059	-0.01522	-0.00088	-0.01942	-0.001
29.5	-0.01128	-0.00059	-0.01521	-0.00088	-0.01939	-0.001
29.25	-0.01129	-0.00059	-0.0152	-0.00088	-0.01935	-0.001
29	-0.0113	-0.00059	-0.01519	-0.00088	-0.01931	-0.00099
29	-0.0113	-0.00059	-0.01519	-0.00088	-0.01931	-0.00099
28.75	-0.01131	-0.00059	-0.01518	-0.00088	-0.01927	-0.00099
28.5	-0.01133	-0.00059	-0.01517	-0.00088	-0.01923	-0.00099
28.25	-0.01135	-0.00059	-0.01517	-0.00088	-0.0192	-0.00099
28	-0.0114	-0.00059	-0.01519	-0.00088	-0.0192	-0.00099
28	-0.0114	-0.00059	-0.01519	-0.00088	-0.0192	-0.00099
27.75	-0.01149	-0.00058	-0.01526	-0.00088	-0.01923	-0.00099
27.5	-0.01159	-0.00058	-0.01534	-0.00087	-0.01927	-0.00099
27.25	-0.0117	-0.00058	-0.01542	-0.00087	-0.01932	-0.00099
27	-0.01181	-0.00058	-0.0155	-0.00087	-0.01936	-0.00098
27	-0.01181	-0.00058	-0.0155	-0.00087	-0.01936	-0.00098
26.75	-0.0119	-0.00058	-0.01556	-0.00087	-0.01939	-0.00098
26.5	-0.01198	-0.00057	-0.01561	-0.00086	-0.01939	-0.00098
26.25	-0.01204	-0.00057	-0.01564	-0.00086	-0.01938	-0.00098
26	-0.01209	-0.00057	-0.01565	-0.00086	-0.01934	-0.00097
26	-0.01209	-0.00057	-0.01565	-0.00086	-0.01934	-0.00097
25.75	-0.01212	-0.00057	-0.01563	-0.00086	-0.01929	-0.00097

25.5	-0.01213	-0.00056	-0.01561	-0.00085	-0.01921	-0.00097
25.25	-0.01215	-0.00056	-0.01558	-0.00085	-0.01914	-0.00096
25	-0.01217	-0.00056	-0.01555	-0.00085	-0.01906	-0.00096
25	-0.01217	-0.00056	-0.01555	-0.00085	-0.01906	-0.00096
24.75	-0.01222	-0.00055	-0.01555	-0.00084	-0.01901	-0.00096
24.5	-0.01228	-0.00055	-0.01556	-0.00084	-0.01896	-0.00095
24.25	-0.01233	-0.00054	-0.01555	-0.00083	-0.0189	-0.00095
24	-0.01237	-0.00054	-0.01553	-0.00083	-0.01881	-0.00094
24	-0.01237	-0.00054	-0.01553	-0.00083	-0.01881	-0.00094
23.75	-0.01239	-0.00053	-0.01548	-0.00082	-0.0187	-0.00093
23.5	-0.01238	-0.00053	-0.0154	-0.00081	-0.01854	-0.00093
23.25	-0.01233	-0.00052	-0.01528	-0.00081	-0.01835	-0.00092
23	-0.01226	-0.00052	-0.01513	-0.0008	-0.01812	-0.00091
23	-0.01226	-0.00052	-0.01513	-0.0008	-0.01812	-0.00091
22.75	-0.01215	-0.00051	-0.01495	-0.0008	-0.01785	-0.00091
22.5	-0.01202	-0.00051	-0.01473	-0.00079	-0.01754	-0.0009
22.25	-0.01186	-0.0005	-0.01449	-0.00078	-0.0172	-0.00089
22	-0.0117	-0.00049	-0.01424	-0.00078	-0.01684	-0.00089
22	-0.0117	-0.00049	-0.01424	-0.00078	-0.01684	-0.00089
21.75	-0.01156	-0.00048	-0.014	-0.00077	-0.0165	-0.00088
21.5	-0.01141	-0.00048	-0.01375	-0.00076	-0.01614	-0.00087
21.25	-0.01125	-0.00047	-0.01348	-0.00075	-0.01576	-0.00086
21	-0.01106	-0.00046	-0.01319	-0.00074	-0.01534	-0.00085
21	-0.01106	-0.00046	-0.01319	-0.00074	-0.01534	-0.00085
20.75	-0.01084	-0.00045	-0.01286	-0.00073	-0.0149	-0.00084
20.5	-0.01059	-0.00044	-0.0125	-0.00072	-0.01442	-0.00083
20.25	-0.0103	-0.00043	-0.01211	-0.00071	-0.0139	-0.00081
20	-0.00998	-0.00042	-0.01167	-0.0007	-0.01334	-0.0008
20	-0.00998	-0.00042	-0.01167	-0.0007	-0.01334	-0.0008
19.75	-0.00963	-0.00041	-0.0112	-0.00069	-0.01275	-0.00079

19.5	-0.00925	-0.0004	-0.01071	-0.00068	-0.01214	-0.00078
19.25	-0.00886	-0.00039	-0.0102	-0.00066	-0.01151	-0.00077
19	-0.00848	-0.00038	-0.0097	-0.00065	-0.0109	-0.00075
19	-0.00848	-0.00038	-0.0097	-0.00065	-0.0109	-0.00075
18.75	-0.00812	-0.00037	-0.00924	-0.00064	-0.01034	-0.00074
18.5	-0.00782	-0.00036	-0.00885	-0.00063	-0.00985	-0.00073
18.25	-0.00758	-0.00035	-0.00851	-0.00062	-0.00944	-0.00072
18	-0.00738	-0.00034	-0.00824	-0.00061	-0.0091	-0.00071
18	-0.00738	-0.00034	-0.00824	-0.00061	-0.0091	-0.00071
17.75	-0.00723	-0.00034	-0.00802	-0.00061	-0.00882	-0.0007
17.5	-0.00711	-0.00033	-0.00784	-0.0006	-0.00859	-0.0007
17.25	-0.00702	-0.00032	-0.0077	-0.00059	-0.0084	-0.00069
17	-0.00694	-0.00032	-0.00759	-0.00059	-0.00825	-0.00068
17	-0.00694	-0.00032	-0.00759	-0.00059	-0.00825	-0.00068
16.75	-0.00688	-0.00031	-0.00749	-0.00058	-0.00812	-0.00068
16.5	-0.00682	-0.00031	-0.0074	-0.00058	-0.008	-0.00067
16.25	-0.00676	-0.0003	-0.00731	-0.00057	-0.00789	-0.00067
16	-0.00671	-0.0003	-0.00723	-0.00057	-0.00777	-0.00066

For 13m excavation depth @1.5m distance from excavation

x=1.5m	100kpa		100kpa		100kpa	
Y	Ux	Uy	Ux	Uy	Ux	Uy
[m]	[m]	[m]	[m]	[m]	[m]	[m]
30	-0.03947	-0.00561	-0.04217	-0.00679	-0.07067	-0.00811
29.75	-0.03876	-0.00561	-0.04189	-0.00679	-0.06967	-0.00811
29.5	-0.03805	-0.00561	-0.04161	-0.00679	-0.06868	-0.00811

29.25	-0.03734	-0.00561	-0.04133	-0.00679	-0.06767	-0.00811
29	-0.03661	-0.00561	-0.04103	-0.00679	-0.06666	-0.00811
29	-0.03661	-0.00561	-0.04103	-0.00679	-0.06666	-0.00811
28.75	-0.03588	-0.00561	-0.04072	-0.00679	-0.06563	-0.00811
28.5	-0.03513	-0.0056	-0.0404	-0.00679	-0.06459	-0.00811
28.25	-0.03439	-0.0056	-0.04008	-0.00679	-0.06354	-0.00811
28	-0.03365	-0.0056	-0.03975	-0.00678	-0.0625	-0.00811
28	-0.03365	-0.0056	-0.03975	-0.00678	-0.0625	-0.00811
27.75	-0.03296	-0.0056	-0.03946	-0.00678	-0.0615	-0.0081
27.5	-0.03228	-0.0056	-0.03917	-0.00678	-0.06051	-0.0081
27.25	-0.03162	-0.00559	-0.03887	-0.00677	-0.05951	-0.00809
27	-0.03095	-0.00559	-0.03855	-0.00677	-0.05849	-0.00809
27	-0.03095	-0.00559	-0.03855	-0.00677	-0.05849	-0.00809
26.75	-0.03029	-0.00558	-0.03819	-0.00676	-0.05745	-0.00808
26.5	-0.02964	-0.00558	-0.0378	-0.00676	-0.05638	-0.00808
26.25	-0.02898	-0.00557	-0.03736	-0.00675	-0.05528	-0.00807
26	-0.02833	-0.00557	-0.03688	-0.00674	-0.05416	-0.00806
26	-0.02833	-0.00557	-0.03688	-0.00674	-0.05416	-0.00806
25.75	-0.02769	-0.00556	-0.03636	-0.00674	-0.053	-0.00806
25.5	-0.02705	-0.00555	-0.03581	-0.00673	-0.05182	-0.00805
25.25	-0.02642	-0.00555	-0.03523	-0.00672	-0.05062	-0.00804
25	-0.02583	-0.00554	-0.03463	-0.00671	-0.04943	-0.00803
25	-0.02583	-0.00554	-0.03463	-0.00671	-0.04943	-0.00803
24.75	-0.02528	-0.00553	-0.03406	-0.0067	-0.04826	-0.00802
24.5	-0.02477	-0.00552	-0.03348	-0.00669	-0.0471	-0.00801
24.25	-0.02427	-0.00551	-0.03288	-0.00668	-0.04594	-0.008
24	-0.02377	-0.0055	-0.03226	-0.00667	-0.04476	-0.00798
24	-0.02377	-0.0055	-0.03226	-0.00667	-0.04476	-0.00798
23.75	-0.02328	-0.00549	-0.03161	-0.00666	-0.04356	-0.00797
23.5	-0.02279	-0.00548	-0.03093	-0.00665	-0.04234	-0.00796

23.25	-0.02228	-0.00547	-0.03021	-0.00663	-0.04109	-0.00795
23	-0.02176	-0.00546	-0.02945	-0.00662	-0.03981	-0.00793
23	-0.02176	-0.00546	-0.02945	-0.00662	-0.03981	-0.00793
22.75	-0.02123	-0.00544	-0.02866	-0.00661	-0.03851	-0.00792
22.5	-0.02069	-0.00543	-0.02783	-0.00659	-0.03719	-0.0079
22.25	-0.02015	-0.00542	-0.02699	-0.00658	-0.03586	-0.00789
22	-0.01962	-0.00541	-0.02616	-0.00656	-0.03454	-0.00787
22	-0.01962	-0.00541	-0.02616	-0.00656	-0.03454	-0.00787
21.75	-0.01913	-0.00539	-0.02535	-0.00655	-0.03327	-0.00785
21.5	-0.01866	-0.00537	-0.02456	-0.00653	-0.03202	-0.00783
21.25	-0.0182	-0.00536	-0.02378	-0.00651	-0.0308	-0.00782
21	-0.01773	-0.00534	-0.023	-0.0065	-0.02959	-0.0078
21	-0.01773	-0.00534	-0.023	-0.0065	-0.02959	-0.0078
20.75	-0.01726	-0.00533	-0.02222	-0.00648	-0.0284	-0.00778
20.5	-0.01677	-0.00531	-0.02143	-0.00646	-0.02722	-0.00776
20.25	-0.01627	-0.00529	-0.02064	-0.00644	-0.02605	-0.00774
20	-0.01574	-0.00528	-0.01983	-0.00642	-0.02488	-0.00771
20	-0.01574	-0.00528	-0.01983	-0.00642	-0.02488	-0.00771
19.75	-0.0152	-0.00526	-0.019	-0.0064	-0.0237	-0.00769
19.5	-0.01463	-0.00524	-0.01816	-0.00638	-0.02252	-0.00767
19.25	-0.01405	-0.00522	-0.01731	-0.00636	-0.02135	-0.00765
19	-0.01346	-0.0052	-0.01646	-0.00634	-0.02018	-0.00763
19	-0.01346	-0.0052	-0.01646	-0.00634	-0.02018	-0.00763
18.75	-0.01289	-0.00518	-0.01565	-0.00632	-0.01905	-0.0076
18.5	-0.01233	-0.00516	-0.01484	-0.00629	-0.01794	-0.00758
18.25	-0.01176	-0.00514	-0.01403	-0.00627	-0.01684	-0.00755
18	-0.01118	-0.00512	-0.01322	-0.00625	-0.01575	-0.00753
18	-0.01118	-0.00512	-0.01322	-0.00625	-0.01575	-0.00753
17.75	-0.01059	-0.0051	-0.01241	-0.00622	-0.01467	-0.0075
17.5	-0.00999	-0.00508	-0.01161	-0.0062	-0.01362	-0.00747

17.25	-0.00941	-0.00506	-0.01084	-0.00617	-0.01261	-0.00745
17	-0.00885	-0.00503	-0.01011	-0.00615	-0.01166	-0.00742
17	-0.00885	-0.00503	-0.01011	-0.00615	-0.01166	-0.00742
16.75	-0.00836	-0.00501	-0.00946	-0.00613	-0.01081	-0.00739
16.5	-0.00796	-0.00499	-0.00892	-0.0061	-0.01009	-0.00737
16.25	-0.00763	-0.00498	-0.00848	-0.00608	-0.0095	-0.00735
16	-0.00737	-0.00496	-0.00813	-0.00606	-0.00903	-0.00733
16	-0.00737	-0.00496	-0.00813	-0.00606	-0.00903	-0.00733
15.75	-0.00717	-0.00494	-0.00785	-0.00604	-0.00865	-0.00731
15.5	-0.00702	-0.00493	-0.00763	-0.00603	-0.00834	-0.00729
15.25	-0.00689	-0.00491	-0.00745	-0.00601	-0.0081	-0.00727
15	-0.00679	-0.0049	-0.00731	-0.006	-0.0079	-0.00725
15	-0.00679	-0.0049	-0.00731	-0.006	-0.0079	-0.00725
14.75	-0.0067	-0.00489	-0.00718	-0.00598	-0.00773	-0.00724
14.5	-0.00662	-0.00488	-0.00707	-0.00597	-0.00757	-0.00723
14.25	-0.00654	-0.00487	-0.00696	-0.00596	-0.00742	-0.00722
14	-0.00646	-0.00486	-0.00685	-0.00595	-0.00728	-0.0072

For 13m excavation @5m distance from excavation

x=5m	100kpa		120kpa		140kpa	
Y	Ux	Uy	Ux	Uy	Ux	Uy
[m]	[m]	[m]	[m]	[m]	[m]	[m]
30	-0.0161	-0.00296	-0.02428	-0.00375	-0.03385	-0.00441
29.75	-0.01615	-0.00296	-0.02424	-0.00375	-0.03378	-0.00441
29.5	-0.01619	-0.00296	-0.0242	-0.00375	-0.03371	-0.00441
29.25	-0.01624	-0.00296	-0.02416	-0.00375	-0.03365	-0.00441

29	-0.01628	-0.00296	-0.02411	-0.00375	-0.03357	-0.0044
29	-0.01628	-0.00296	-0.02411	-0.00375	-0.03357	-0.0044
28.75	-0.01633	-0.00296	-0.02407	-0.00375	-0.0335	-0.0044
28.5	-0.01638	-0.00296	-0.02403	-0.00375	-0.03343	-0.0044
28.25	-0.01644	-0.00296	-0.024	-0.00375	-0.03336	-0.0044
28	-0.01653	-0.00296	-0.02399	-0.00375	-0.03331	-0.0044
28	-0.01653	-0.00296	-0.02399	-0.00375	-0.03331	-0.0044
27.75	-0.01665	-0.00295	-0.02402	-0.00375	-0.03329	-0.0044
27.5	-0.01679	-0.00295	-0.02407	-0.00374	-0.03329	-0.0044
27.25	-0.01693	-0.00295	-0.02411	-0.00374	-0.03328	-0.0044
27	-0.01706	-0.00295	-0.02414	-0.00374	-0.03326	-0.00439
27	-0.01706	-0.00295	-0.02414	-0.00374	-0.03326	-0.00439
26.75	-0.01718	-0.00294	-0.02416	-0.00374	-0.03321	-0.00439
26.5	-0.01727	-0.00294	-0.02416	-0.00373	-0.03314	-0.00439
26.25	-0.01733	-0.00294	-0.02414	-0.00373	-0.03304	-0.00438
26	-0.01738	-0.00294	-0.02409	-0.00373	-0.03292	-0.00438
26	-0.01738	-0.00294	-0.02409	-0.00373	-0.03292	-0.00438
25.75	-0.01739	-0.00293	-0.02402	-0.00372	-0.03277	-0.00438
25.5	-0.01739	-0.00293	-0.02394	-0.00372	-0.03259	-0.00437
25.25	-0.01738	-0.00292	-0.02384	-0.00371	-0.03239	-0.00437
25	-0.01737	-0.00292	-0.02374	-0.00371	-0.03219	-0.00436
25	-0.01737	-0.00292	-0.02374	-0.00371	-0.03219	-0.00436
24.75	-0.01738	-0.00291	-0.02367	-0.0037	-0.032	-0.00436
24.5	-0.01739	-0.00291	-0.0236	-0.0037	-0.0318	-0.00435
24.25	-0.0174	-0.0029	-0.0235	-0.00369	-0.03157	-0.00434
24	-0.01738	-0.0029	-0.02339	-0.00368	-0.03131	-0.00434
24	-0.01738	-0.0029	-0.02339	-0.00368	-0.03131	-0.00434
23.75	-0.01733	-0.00289	-0.02324	-0.00368	-0.03101	-0.00433
23.5	-0.01725	-0.00288	-0.02306	-0.00367	-0.03066	-0.00432
23.25	-0.01714	-0.00288	-0.02284	-0.00366	-0.03027	-0.00431

23	-0.017	-0.00287	-0.02258	-0.00365	-0.02982	-0.0043
23	-0.017	-0.00287	-0.02258	-0.00365	-0.02982	-0.0043
22.75	-0.01682	-0.00286	-0.02228	-0.00364	-0.02932	-0.0043
22.5	-0.01662	-0.00285	-0.02196	-0.00364	-0.02878	-0.00429
22.25	-0.0164	-0.00285	-0.02161	-0.00363	-0.02821	-0.00428
22	-0.01618	-0.00284	-0.02125	-0.00362	-0.02762	-0.00427
22	-0.01618	-0.00284	-0.02125	-0.00362	-0.02762	-0.00427
21.75	-0.01598	-0.00283	-0.02091	-0.00361	-0.02704	-0.00426
21.5	-0.01579	-0.00282	-0.02057	-0.00359	-0.02646	-0.00424
21.25	-0.01559	-0.00281	-0.02021	-0.00358	-0.02585	-0.00423
21	-0.01537	-0.0028	-0.01983	-0.00357	-0.02523	-0.00422
21	-0.01537	-0.0028	-0.01983	-0.00357	-0.02523	-0.00422
20.75	-0.01513	-0.00278	-0.01943	-0.00356	-0.02458	-0.00421
20.5	-0.01486	-0.00277	-0.01899	-0.00355	-0.0239	-0.00419
20.25	-0.01457	-0.00276	-0.01852	-0.00353	-0.02318	-0.00418
20	-0.01425	-0.00275	-0.01802	-0.00352	-0.02243	-0.00416
20	-0.01425	-0.00275	-0.01802	-0.00352	-0.02243	-0.00416
19.75	-0.01389	-0.00274	-0.01747	-0.00351	-0.02163	-0.00415
19.5	-0.01351	-0.00272	-0.01688	-0.00349	-0.0208	-0.00413
19.25	-0.01311	-0.00271	-0.01627	-0.00348	-0.01994	-0.00412
19	-0.0127	-0.0027	-0.01564	-0.00346	-0.01906	-0.0041
19	-0.0127	-0.0027	-0.01564	-0.00346	-0.01906	-0.0041
18.75	-0.0123	-0.00268	-0.01503	-0.00345	-0.01819	-0.00408
18.5	-0.01189	-0.00267	-0.0144	-0.00343	-0.0173	-0.00406
18.25	-0.01146	-0.00265	-0.01375	-0.00341	-0.01641	-0.00405
18	-0.01102	-0.00264	-0.01309	-0.00339	-0.0155	-0.00403
18	-0.01102	-0.00264	-0.01309	-0.00339	-0.0155	-0.00403
17.75	-0.01055	-0.00262	-0.01242	-0.00338	-0.01459	-0.00401
17.5	-0.01006	-0.00261	-0.01173	-0.00336	-0.01368	-0.00399
17.25	-0.00958	-0.00259	-0.01106	-0.00334	-0.01279	-0.00397

17	-0.0091	-0.00257	-0.01042	-0.00332	-0.01195	-0.00395
17	-0.0091	-0.00257	-0.01042	-0.00332	-0.01195	-0.00395
16.75	-0.00868	-0.00256	-0.00984	-0.0033	-0.01119	-0.00393
16.5	-0.00831	-0.00254	-0.00935	-0.00329	-0.01054	-0.00391
16.25	-0.00802	-0.00253	-0.00894	-0.00327	-0.01001	-0.00389
16	-0.00779	-0.00252	-0.00862	-0.00325	-0.00957	-0.00387
16	-0.00779	-0.00252	-0.00862	-0.00325	-0.00957	-0.00387
15.75	-0.00761	-0.0025	-0.00836	-0.00324	-0.00922	-0.00386
15.5	-0.00746	-0.00249	-0.00815	-0.00323	-0.00893	-0.00385
15.25	-0.00734	-0.00248	-0.00798	-0.00322	-0.00869	-0.00383
15	-0.00724	-0.00247	-0.00784	-0.00321	-0.0085	-0.00382
15	-0.00724	-0.00247	-0.00784	-0.00321	-0.0085	-0.00382
14.75	-0.00716	-0.00246	-0.00771	-0.0032	-0.00832	-0.00381
14.5	-0.00708	-0.00246	-0.0076	-0.00319	-0.00816	-0.0038
14.25	-0.007	-0.00245	-0.00749	-0.00318	-0.00801	-0.00379
14	-0.00692	-0.00244	-0.00737	-0.00317	-0.00786	-0.00378

For 13m excavation @7.5m distance from excavation

x=7.5m	100kpa		120kpa		140kpa	
Y	Ux	Uy	Ux	Uy	Ux	Uy
[m]	[m]	[m]	[m]	[m]	[m]	[m]
30	-0.01388	-0.00174	-0.01824	-0.00215	-0.0241	-0.00262
29.75	-0.01389	-0.00174	-0.01825	-0.00215	-0.02409	-0.00262
29.5	-0.01391	-0.00174	-0.01826	-0.00215	-0.02409	-0.00262
29.25	-0.01392	-0.00174	-0.01827	-0.00215	-0.02409	-0.00262
29	-0.01393	-0.00174	-0.01829	-0.00215	-0.02408	-0.00262
29	-0.01393	-0.00174	-0.01829	-0.00215	-0.02408	-0.00262
28.75	-0.01395	-0.00174	-0.0183	-0.00215	-0.02408	-0.00262
28.5	-0.01397	-0.00174	-0.01831	-0.00215	-0.02407	-0.00262
28.25	-0.014	-0.00174	-0.01834	-0.00215	-0.02408	-0.00262
28	-0.01405	-0.00174	-0.01838	-0.00215	-0.02411	-0.00262
28	-0.01405	-0.00174	-0.01838	-0.00215	-0.02411	-0.00262
27.75	-0.01414	-0.00173	-0.01847	-0.00215	-0.02417	-0.00262
27.5	-0.01425	-0.00173	-0.01857	-0.00215	-0.02425	-0.00262
27.25	-0.01436	-0.00173	-0.01867	-0.00215	-0.02433	-0.00261
27	-0.01447	-0.00173	-0.01876	-0.00214	-0.0244	-0.00261
27	-0.01447	-0.00173	-0.01876	-0.00214	-0.0244	-0.00261
26.75	-0.01456	-0.00173	-0.01884	-0.00214	-0.02446	-0.00261
26.5	-0.01464	-0.00172	-0.01891	-0.00214	-0.0245	-0.00261
26.25	-0.0147	-0.00172	-0.01895	-0.00214	-0.02451	-0.0026
26	-0.01475	-0.00172	-0.01897	-0.00213	-0.0245	-0.0026
26	-0.01475	-0.00172	-0.01897	-0.00213	-0.0245	-0.0026
25.75	-0.01478	-0.00172	-0.01897	-0.00213	-0.02447	-0.0026
25.5	-0.01479	-0.00171	-0.01896	-0.00213	-0.02442	-0.0026

25.25	-0.01481	-0.00171	-0.01894	-0.00212	-0.02437	-0.00259
25	-0.01484	-0.00171	-0.01893	-0.00212	-0.02432	-0.00259
25	-0.01484	-0.00171	-0.01893	-0.00212	-0.02432	-0.00259
24.75	-0.01489	-0.0017	-0.01895	-0.00212	-0.02429	-0.00258
24.5	-0.01496	-0.0017	-0.01897	-0.00211	-0.02426	-0.00258
24.25	-0.01502	-0.00169	-0.01898	-0.00211	-0.02422	-0.00257
24	-0.01507	-0.00169	-0.01897	-0.0021	-0.02416	-0.00257
24	-0.01507	-0.00169	-0.01897	-0.0021	-0.02416	-0.00257
23.75	-0.0151	-0.00168	-0.01894	-0.00209	-0.02407	-0.00256
23.5	-0.0151	-0.00168	-0.01887	-0.00209	-0.02394	-0.00255
23.25	-0.01507	-0.00167	-0.01878	-0.00208	-0.02377	-0.00255
23	-0.01501	-0.00167	-0.01865	-0.00208	-0.02357	-0.00254
23	-0.01501	-0.00167	-0.01865	-0.00208	-0.02357	-0.00254
22.75	-0.01493	-0.00166	-0.01849	-0.00207	-0.02332	-0.00253
22.5	-0.01482	-0.00165	-0.0183	-0.00206	-0.02304	-0.00253
22.25	-0.01469	-0.00165	-0.0181	-0.00206	-0.02274	-0.00252
22	-0.01457	-0.00164	-0.01789	-0.00205	-0.02243	-0.00251
22	-0.01457	-0.00164	-0.01789	-0.00205	-0.02243	-0.00251
21.75	-0.01447	-0.00163	-0.01771	-0.00204	-0.02213	-0.0025
21.5	-0.01437	-0.00163	-0.01752	-0.00203	-0.02183	-0.00249
21.25	-0.01426	-0.00162	-0.01733	-0.00202	-0.02152	-0.00248
21	-0.01414	-0.00161	-0.01711	-0.00201	-0.02117	-0.00247
21	-0.01414	-0.00161	-0.01711	-0.00201	-0.02117	-0.00247
20.75	-0.01399	-0.0016	-0.01687	-0.002	-0.0208	-0.00246
20.5	-0.01381	-0.00159	-0.0166	-0.00199	-0.0204	-0.00245
20.25	-0.0136	-0.00158	-0.01629	-0.00198	-0.01995	-0.00244
20	-0.01336	-0.00157	-0.01596	-0.00197	-0.01947	-0.00243
20	-0.01336	-0.00157	-0.01596	-0.00197	-0.01947	-0.00243
19.75	-0.01309	-0.00156	-0.01558	-0.00196	-0.01894	-0.00242
19.5	-0.01279	-0.00155	-0.01517	-0.00195	-0.01836	-0.00241

19.25	-0.01246	-0.00154	-0.01474	-0.00194	-0.01776	-0.00239
19	-0.01213	-0.00153	-0.01429	-0.00193	-0.01713	-0.00238
19	-0.01213	-0.00153	-0.01429	-0.00193	-0.01713	-0.00238
18.75	-0.0118	-0.00152	-0.01385	-0.00191	-0.0165	-0.00237
18.5	-0.01147	-0.00151	-0.01339	-0.0019	-0.01586	-0.00235
18.25	-0.01111	-0.00149	-0.01292	-0.00189	-0.01519	-0.00233
18	-0.01073	-0.00148	-0.01241	-0.00187	-0.0145	-0.00232
18	-0.01073	-0.00148	-0.01241	-0.00187	-0.0145	-0.00232
17.75	-0.01033	-0.00147	-0.01188	-0.00186	-0.01378	-0.0023
17.5	-0.0099	-0.00145	-0.01133	-0.00184	-0.01305	-0.00229
17.25	-0.00947	-0.00144	-0.01077	-0.00183	-0.01232	-0.00227
17	-0.00905	-0.00142	-0.01023	-0.00181	-0.01162	-0.00225
17	-0.00905	-0.00142	-0.01023	-0.00181	-0.01162	-0.00225
16.75	-0.00867	-0.00141	-0.00974	-0.0018	-0.01099	-0.00224
16.5	-0.00834	-0.0014	-0.00932	-0.00178	-0.01044	-0.00222
16.25	-0.00808	-0.00139	-0.00897	-0.00177	-0.00998	-0.00221
16	-0.00787	-0.00138	-0.00868	-0.00176	-0.0096	-0.00219
16	-0.00787	-0.00138	-0.00868	-0.00176	-0.0096	-0.00219
15.75	-0.0077	-0.00137	-0.00845	-0.00175	-0.00929	-0.00218
15.5	-0.00757	-0.00136	-0.00827	-0.00174	-0.00904	-0.00217
15.25	-0.00746	-0.00135	-0.00812	-0.00173	-0.00883	-0.00216
15	-0.00737	-0.00134	-0.00799	-0.00172	-0.00866	-0.00215
15	-0.00737	-0.00134	-0.00799	-0.00172	-0.00866	-0.00215
14.75	-0.00729	-0.00133	-0.00787	-0.00171	-0.0085	-0.00214
14.5	-0.00721	-0.00133	-0.00777	-0.00171	-0.00835	-0.00214
14.25	-0.00714	-0.00132	-0.00766	-0.0017	-0.00822	-0.00213
14	-0.00706	-0.00132	-0.00756	-0.00169	-0.00808	-0.00212

REFERENCES

Eric Lindquist, Rob Jameson (2011) "secant pile shoring development in design and construction" 36th annual conference of deep foundation, Boston.

Ali Saleh (2014) "Analysis and design of circular shaft using Finite Element Method." American University of Sharjah, United Emirates.

Clough, G., & O'Rourke, T. (1990). Construction induced movements of in-situ walls. Proceeding of ASCE Special Conference on Design and Performance of Earth Retaining Structures, (pp. 439-470). Cornell University, New York.

Hashash, M. (1992). Analysis of Deep Excavation in Clay. MIT, Dept. of Civil Engineering. Cambridge, MA.

Balasubramaniam, A., Bergado, D., & Sutabutr, T. (1994). Deformation analysis of deep excavation in Bangkok subsoils. Proceedings of the Thirteen International Conference on Soil Mechanics and Foundation Engineering, 13(2), pp. 909-914.

Chavada Jitesh, Desai A.K., Solanki C.H. (2015) "Parametric study of pile wall used as retention system for deep excavations" international journal of soil mechanics and foundation, volume 1: issue 2

W. Allen Marr and Martin Hawkes (2010) "Displacement-Based Design for Deep Excavations." Earth Retention Conference 3: pp. 82-100.

Hilary Term (2014) "Advanced Finite Element Analysis of Deep Excavation Case Histories." Department of engineering science university of oxford"

William Bjureland (2013) "Analysis of deep excavations using the mobilized strength design (MSD) method." Division of Soil- and Rock Mechanics Department of Civil, Architectural and the Built Environment, thesis.

L.Tony Chen (2013) "A case History of Deep excavation in Doha." Seventh international Conference, Chicago.

David G. Zapata-Medina (2007)"Semi-Empirical Method for Designing Excavation Support Systems Based on Deformation Control "University of Kentucky Master's Theses, Paper 468.

Grabe J. (2010) "Sheet piling handbook design" Hamburg, German.

RJ Finno, LS Bryson (2002) "Response of building adjacent to stiff excavation support system in soft clay." Journal of Performance of Constructed Facilities.

Aiza Malik (2015) "Geotechnical Statistical Evaluation of Lahore Site Data and Deep Excavation Design". Civil and Environmental Engineering Master's Project Reports, Paper 13.

A.Siemińska-Lewandowska & M. Mitew-Czajewska (2011) "The study of displacements of diaphragm walls built in Warsaw Quaternary soils" Geotechnical Aspects of Underground Construction in Soft Ground, Taylor & Francis Group, London, ISBN 978-0-415-68367-8.

A.S.Osman and M.D. Bolton (2004) "Ground Movement Predictions for Braced Excavation in Undrained Clay" Journal of Geotechnical and Geoenvironmental Engineering, Vol. 132, No. 4.

A.T.C. Goh, K.S.Wong, C.I.Teh & D.Wen (2003) "Pile Response Adjacent to Braced Excavation" Journal of Geotechnical and Geoenvironmental Engineering, Vol. 129, No. 4.

B.C.B. Hsiung (2008) "A case studies on the behavior of a deep excavation in sand" Computers and Geotechnics Vol. 36, pp.665–675.

Bowles, J.E. (1996). "Foundation Analysis and Design". Fifth Edition, McGraw-Hill, New York. Fourth Edition, 1988.

Geotechnics Group, Institute for Soil Mechanics and Foundation Engineering, Graz University of Technology, Austria.

H.Popa, A. Marcu & L. Batali (2008) "Numerical modelling and experimental measurements for a retaining wall of a deep excavation in Bucharest, Romania" Geotechnical Aspects of Underground Construction in Soft Ground, Taylor & Francis Group, London, ISBN 978-0-415-48475-6.

Intsiful & Sekyi K.(2015) "Deformation-based Excavation Support System Design Method". Theses and Dissertations, Civil Engineering, Paper 29.

J. H. Wang; Z. H. Xu; and W. D. Wang (2010)"Wall and Ground Movements due to Deep Excavations in Shanghai Soft Soils" journal of geotechnical and geoenvironmental engineering Vol. 136: pp. 985-994.

J. Josifovski 1, S. Gjorgjevski and M. Jovanovski (2011) " Deep Excavation with Multi Anchored Diaphragm Wall" Proceedings of the 15th European Conference on Soil Mechanics and Geotechnical Engineering oi:10.3233/978-1-60750-801-4-1485.

J.Roboski & R.J. Finno (2005) “Distributions of Ground Movements Parallel to Deep Excavations in Clay" paper submitted to the Canadian Geotechnical Journal.

J.T. Blackburn and R.J. Finno (2006) “Three-dimensional effects observed in an internally braced excavation in soft clay" Paper submitted to the Journal of Geotechnical and Geoenvironmental Engineering.

K.H. Goh & R.J. Mair (2011) “The response of buildings to movements induced by deep excavations" Geotechnical Aspects of Underground Construction in Soft Ground Taylor & Francis Group, London, ISBN 978-0-415-68367-8.

K.H. Yang and C.N.Liu(2007) " Finite Element Analysis Of Earth Pressures for Narrow Retaining Walls" Journal of GeoEngineering, Vol. 2, No. 2, pp. 43-52.

Garvin, R., & Boward, J. (1992). Using slurry walls to protect a historic building: a case study. Slurry walls: Design, Construction, and Quality Control ASTM Special Topic Publication 1129 , 117-127.

Peck R.(1969) "Deep excavations and tunneling in soft ground" Proceedings of the 7th International Conference on Soil Mechanics, pp. 225-290.

P.J. Sabatini, D.G. Pass, R.C. Bachus (1999) " Geotechnical Engineering Circular No. 4 Ground Anchors and Anchored Systems" US Dept. of transportation, FHWA-IF-99-015.

M.A. Nikolinakou, A. J. Whittle, S.Savidis and U.Schran(2011) "Prediction and Interpretation of the Performance of a Deep Excavation in Berlin Sand" Journal of Geotechnical and Geoenvironmental Engineering, Vol. 137, No. 11.

M. Korff & R.J.Mair (2013) " Response of piled buildings to deep excavations in soft soils" Proceedings of the 18th International Conference on Soil Mechanics and Geotechnical Engineering, Paris.

Tianteng Zhou (2015) " 3D FEM Analysis For Sequential Excavation" Delt University of Technology Master's thesis.

V.R. Godavarthi, D. Mallavalli, R. Peddi, N.Katragadda, and P.Mulpuru (2011) " Contiguous Pile Wall as a Deep Excavation Supporting System" Leonardo Electronic Journal of Practices and Technologies ISSN 1583-1078, pp. 144-160.

Yuepeng Dong(2013) " Advanced Finite Element Analysis of Deep Excavation Case Histories" University of Oxford PHD theses, Dept. of engineering science.

Powrie, W., & Li, E. (1991). Finite element analysis of an in-situ wall propped at formation level. Geotechnique , 41 (4), 499-514.

Tewodros Fekadu (2010) "Analysis and parametric study of deep excavation with diaphragm wall using finite element based software" Addis Ababa University Master's Theses, Dept. of Civil Engineering. Addis Ababa, Ethiopia.

Poul V. Lade (1989) "Single-Hardening Model With Application to Normally Consolidated Clay" Journal of Geotechnical Engineering, Vol. 116, No. 3.

R.Catzenbach, (2003), DIN-4094Bb1;1990-12

Konstantakos, D., Whittle, A., Regalado, C., & Scharner, B. (2004). Control of ground movements for a multi-level-anchored, diaphragm wall during excavation. Proceedings: Fifth International Conference on Case Histories in Geotechnical Engineering. New York, NY.

R.J. Finno and L.S. Bryson (2002) " Response of Building Adjacent to Stiff Excavation Support System in Soft Clay" Journal of Performance of Constructed Facilities, Vol. 16, No. 1.

Raithel, M., Gebreselassie, B., Müller, S., & Pahl, F. (2005). Design and Numerical Investigations of a Deep Excavation for a Tunnel Entrance Pit. 16th International Conference on Soil Mechanics and Geotechnical Engineering. Osaka, Japan.

Surarak, C. (2010). Geotechnical Aspects of the Bangkok MRT Blue Line Project. Ph.D. Thesis, Griffith University, Australia.

Teferra, A. (1992). "Foundation Engineering" Addis Ababa: Addis Ababa University Press.